NMR Residual Dipolar Couplings as Probes of Biomolecular Dynamics

Joel R. Tolman* and Ke Ruan

Department of Chemistry, Johns Hopkins University, 3400 North Charles Street, Baltimore, Maryland 21218

Received July 29, 2005 (Revised Manuscript Received February 21, 2006)

Contents

1. Introduction 1720
2. Relationship of Residual Dipolar Couplings to Molecular Structure and Dynamics 1721
   2.1. Anisotropic Averaging of the Dipolar Interaction 1721
   2.2. Rigid Molecules 1721
   2.3. Flexible Molecules 1722
3. Molecular Alignment 1724
   3.1. Methods for Inducing Molecular Alignment 1724
   3.2. Experimental Determination of the Alignment Tensor 1724
   3.3. Assessing the Independence of RDC Data Acquired in Multiple Alignment Media 1725
4. Biomolecular Dynamics from Residual Dipolar Couplings 1726
   4.1. Domain Motions 1727
   4.2. Local or Segmental Motions 1728
   4.3. Generalized Order Parameters from Residual Dipolar Couplings 1729
   4.4. Peptide Plane Dynamics 1732
   4.5. Ensemble Simulated Annealing 1733
   4.6. Side-Chain Dynamics 1734
5. Future Perspectives 1734
6. Acknowledgments 1735
7. References 1735

Joel R. Tolman was born in Salt Lake City, Utah, and raised in New Jersey, receiving his bachelor's degree from Rutgers University in 1990. He earned his Ph.D. in Chemistry from Yale University under the direction of Professor James H. Prestegard in 1997. After assuming postdoctoral research positions with Prof. Lewis E. Kay and Prof. Geoffrey Bodenhausen, he accepted a position at the Johns Hopkins University in 2002 as an Assistant Professor of Chemistry. At present, his research is focused on the development of residual dipolar coupling based approaches to the characterization of protein structural dynamics and NMR spectroscopic investigations of protein–protein interactions involved in polyubiquitination.

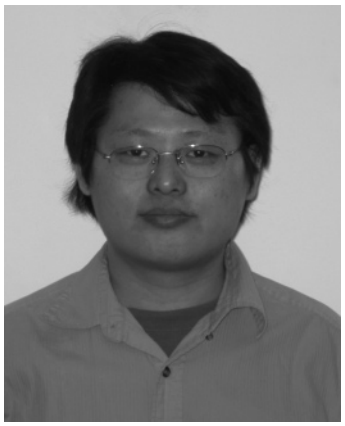

Ke Ruan was born and raised in Anhui, P. R. China, and received his B.S. and M.S. in chemistry from Peking University. He is currently a Ph.D. student in chemistry at the Johns Hopkins University under the direction of Prof. Joel Tolman. His research is focused on developing RDC-based methods to study protein structures and dynamics.

1. Introduction

Since the first applications of residual dipolar couplings (RDCs) to biomolecular systems approximately a decade ago, RDCs have rapidly emerged as a standard tool for the characterization of structure in solution. However, their application to the study of biomolecular dynamics has developed much more slowly, in large part due to the additional difficulties associated with their interpretation. So why develop techniques for studying dynamics using RDCs when there are a number of mature spin relaxation based techniques[1−7] that can be used to study motions on the subnanosecond as well as on the microsecond to millisecond time scales? The answer is twofold. First, RDCs can provide detailed structural dynamic information at atomic resolution, which informs directly on the spatial nature of conformational fluctuations of biomolecules. Second, RDCs are sensitive to motions spanning the picosecond to millisecond time scales and therefore can detect motions occurring on the intermediate nanosecond−microsecond time scale, which may not be picked up by existing spin relaxation based approaches. In short, RDCs offer a view of dynamic processes that is very complementary to other NMR spectroscopic approaches.

Techniques for studying dynamics using RDCs are still evolving. The most straightforward applications are to molecules that are composed of domains or segments that

* To whom correspondence should be addressed. Phone: (410) 516-8022. Fax: (410) 516-8420. E-mail: tolman@jhu.edu.

10.1021/cr040429z CCC: $59.00
Published on Web 04/08/2006

can individually be assumed to be rigid. The measurement of RDCs corresponding to each individual segment can allow the relative mobility of segments to be established. The availability of numerous different media for inducing molecular alignment provides for the acquisition of extensive sets of RDCs such that it is now feasible to consider the determination of a set of conformations of a biomolecule rather than a single structure. These multialignment RDC studies also have enabled the determination of dipolar generalized order parameters, which complement their spin relaxation derived counterparts due to their sensitivity to broader motional time scales.

There are now a number of reviews that address the application of residual dipolar coupling methodology to the determination of biomolecular structure and dynamics.[8−27] We do not attempt a comprehensive review of the field here but rather focus on a discussion of the aspects important for the acquisition of RDCs in multiple alignment media and the interpretation of RDCs in terms of structure and dynamics, and we survey the various techniques now available for probing biomolecular dynamics.

2. Relationship of Residual Dipolar Couplings to Molecular Structure and Dynamics

The relationship of measured anisotropic NMR parameters such as dipolar or quadrupolar couplings to molecular structural (and dynamic) properties have long been recognized and the corresponding theoretical frameworks established.[28−52] Because biomolecular applications using a wide array of different alignment media have become commonplace, there have been further developments in the analysis of residual tensorial properties measured in anisotropic media.[8,9,15,26] We will focus attention at present to highlighting the basis for the sensitivity of RDCs to molecular structural and dynamic properties, and the attendant difficulties in separating these effects. The notation utilized is deliberately consistent with previous work, to which the reader is referred for more extensive discussion.[9,15] Finally, we note that although the discussion is restricted for simplicity to RDCs, it is straightforward to extend these results to the residual chemical shift anisotropy or quadrupolar coupling interactions.

2.1. Anisotropic Averaging of the Dipolar Interaction

The direct magnetic interaction between a pair of nuclear magnetic moments gives rise to the nuclear dipole−dipole interaction. Although a full description of the dipolar interaction is complicated, at high magnetic fields it is only necessary to consider a simplified version. In the laboratory frame, the truncated dipolar Hamiltonian for a weakly coupled nuclear spin pair is (units of Hz)[53,54]

$$H_{ij}^{\mathrm{D}}(t) = -\left(\frac{\mu_0}{4\pi}\right)\frac{\gamma_i\gamma_j h}{2\pi^2 r_{ij}^{\ 3}(t)}\mathbf{I}_{iz}\mathbf{I}_{jz}P_2(\cos\theta_{ij}(t)) \qquad (1)$$

where r_{ij} is the internuclear distance between spins, γ_i and γ_j are the gyromagnetic ratios of spins i and j, respectively, the $\mathbf{I}_{kz}$ are spin angular momentum operators, and $P_2(\cos\theta_{ij}(t))$ is the second rank Legendre function, which depends on the angle θ_{ij} subtended by the magnetic field and the ijth internuclear vector.

In the solution state, the time dependence of the dipolar Hamiltonian is due to overall molecular reorientation as well as bond vibrations and internal motions. Under normal solution conditions in which the molecule does not assume any preferential orientation relative to the magnetic field, the angular term $P_2(\cos\theta_{ij}(t))$ will average to zero. Hence, RDCs are not normally observed in the solution NMR spectrum. However, if the isotropy of molecular orientation can be perturbed, then small residuals of the incompletely averaged dipolar interaction will manifest in the spectrum as a contribution to the splittings of lines. Under anisotropic solution conditions, the following expression can be used to describe the residual dipolar coupling:

$$D_{ij}^{\mathrm{res}} = -\left(\frac{\mu_0}{4\pi}\right)\frac{\gamma_i\gamma_j h}{2\pi^2 r_{ij,\mathrm{eff}}^{\ 3}}\langle P_2(\cos\theta_{ij}(t))\rangle \qquad (2)$$

in which the angle brackets denote that the time average has been taken. In addition, an effective internuclear distance, $r_{ij,\mathrm{eff}}$, has been introduced to represent its vibrationally corrected value. The justification for separation of terms for distance and angular averaging rests on the assumption that these processes occur on very different time scales, allowing their averages to be computed independently.[55] As seen in eq 2, the interpretation of RDCs in terms of structure or dynamics rests on the means by which the average $\langle P_2(\cos\theta_{ij}(t))\rangle$ is partitioned into its various contributing factors. From an experimental standpoint, there are two routes by which to proceed: either make several RDC measurements corresponding to different dipolar interactions that have a rigid structural relationship to one another or measure RDCs under different aligning conditions.

2.2. Rigid Molecules

It was first recognized by Saupe[36,56] that for a rigid molecule one can expand the angular average $\langle P_2(\cos\theta_{ij}(t))\rangle$ appearing in eq 2 into a sum of geometric terms describing the orientation of the internuclear vector within the molecule and corresponding averages that describe the nature of the ordering of the entire molecule.[35]

$$\langle P_2(\cos\theta_{ij})\rangle = \sum_{kl=xyz}\mathbf{S}_{kl}\cos(\alpha_k^{ij})\cos(\alpha_l^{ij}) \qquad (3)$$

The rigid molecular geometry is described using direction cosines, in which α_n^{ij} subtends the angle between the ijth internuclear vector and the n-axis within an arbitrarily placed set of Cartesian coordinate axes (Figure 1). The terms $\mathbf{S}_{kl}$,

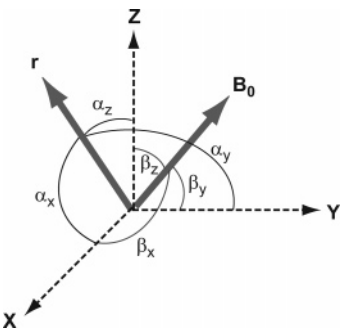

Figure 1. Depiction of the direction cosines describing the orientation of the ijth internuclear vector (α_n^{ij}) and the magnetic field vector (β_n) relative to an arbitrary molecule-fixed coordinate system.

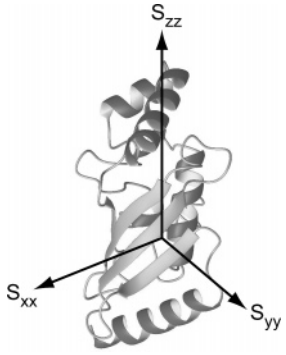

Figure 2. The principal axes of alignment are fixed to the molecule and specify the direction of highest (S_{zz}) and lowest ordering (S_{xx}) relative to the magnetic field.

which describe the ordering of the molecule, are collected into a Cartesian 3 × 3 tensor referred to as the order tensor. The elements of the order tensor are time averages over functions that depend on the orientation of the magnetic field relative to an arbitrarily molecule fixed coordinate system,

$$\mathbf{S}_{kl} = \left\langle \frac{3}{2}\cos(\beta_k(t))\cos(\beta_l(t)) - \frac{1}{2}\delta_{kl} \right\rangle \tag{4}$$

where the time-dependent angles $\beta_n(t)$ describe the orientation of the magnetic field (Figure 1) and the δ_{kl} represent the Kronecker delta function. Because the Saupe order tensor is both symmetric and traceless, it has only five independent elements and can always be diagonalized. Upon diagonalization, the magnitude and asymmetry of alignment are contained in the eigenvalues, and the orientation of the principal axis system (PAS) of molecular alignment is specified by the transformation matrix formed from the eigenvectors. Specification of the PAS of order (alignment) amounts to the determination of a set of coordinate axes fixed to the molecule (Figure 2). The positioning of the principal axes is such that the *z*-axis points in the direction of maximum order relative to the magnetic field and the *x*-axis points in the direction of least order relative to the magnetic field, subject to maintenance of orthogonality of the three axes. Due to the traceless nature of the order tensor, only two magnitudes need be specified. Typically reported are the degree of ordering of the principal axis (S_{zz}) and the difference in ordering along the *x* and *y* axes (η). It is common that the residual dipolar coupling is expressed in the PAS of molecular alignment,

$$D_{ij}^{\text{res}} = -\left(\frac{\mu_0}{4\pi}\right)\frac{\gamma_i\gamma_j h}{2\pi^2 r_{ij}^{\ 3}} S_{zz}\left\{\frac{1}{2}(3\cos^2\theta - 1) + \frac{1}{2}\eta\sin^2\theta\cos 2\phi\right\} \tag{5}$$

in which the asymmetry, η, is defined as $(S_{xx} - S_{yy})/S_{zz}$. It is usually assumed that the PAS of alignment forms a right-handed coordinate system with principal axes chosen according to $|S_{zz}| \geq |S_{yy}| \geq |S_{xx}|$. These conditions constrain η to lie between values of 0 and 1. From eq 5, it is clear that a given RDC measurement, D_{ij}^{res}, will not correspond to a unique orientation of the internuclear vector. Indeed a single measured RDC will correspond to a continuum of orientations that lie on the surface of a flattened cone as shown in Figure 3. The lack of a one-to-one relationship between a measured RDC and the internuclear vector orientation poses additional challenges for the interpretation of RDC data in terms of molecular structural and dynamic parameters.

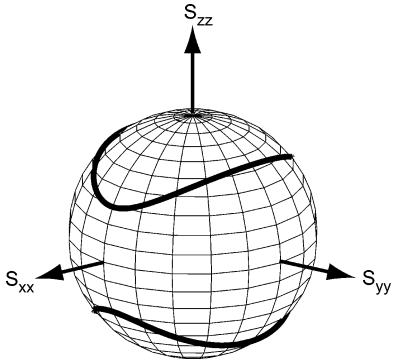

Figure 3. A single measured RDC will correspond to a continuum of possible internuclear vector orientations, as indicated by the thick line. In general, the possible internuclear vector orientations will appear as a flattened cone relative to the principal axes of alignment.

2.3. Flexible Molecules

There is no single recipe for accounting for the effects of dynamics on measured RDCs. In general, an observed RDC arises from a weighted average over all molecular conformations, each of which align differently relative to the magnetic field. This can be expressed as follows:

$$D_{ij}^{\text{res}} = \sum_{\Gamma} p(\Gamma) D_{ij}^{res}(\Gamma) \tag{6}$$

where Γ refers to a specific conformation, $p(\Gamma)$ refers to the population fraction of this conformation, and $D_{ij}^{\text{res}}(\Gamma)$ is the RDC corresponding to this conformation. As has been pointed out, this is likely an appropriate framework for interpretation of RDCs measured for unfolded proteins.[57,58] However, for folded proteins or cases in which the molecule exhibits segmental rigidity, more detailed methods exist for characterizing molecular dynamics using RDCs. The approaches can be separated into three distinct categories, of which the first is the use of a specific motional model. An example of this is the use of the 1D ortho-GAF model[59,60] to characterize peptide plane motions as discussed in section 4. We refer the interested reader to the work of Bouvignies et al.[61] and Deschamps et al.[62] for a detailed treatment of the effects of specific motional models on the averaging of RDCs. The other two cases are discussed below.

There are often cases in which segments of a biomolecule can be reasonably assumed to be rigid. In these cases, each rigid segment can in effect be treated as a separate molecule with a characteristic order (alignment) tensor.[8,15,63,64] Diagonalization of each separate order tensor provides information about the relative orientation and dynamics of the separate segments. By insistence that the principal axes must coincide for different segments, the mean relative orientation of different segments may be established, subject to the possibility of distortions due to dynamics. For segments that are rigidly related to one another, one expects determination of identical principal order parameters, reflecting a common degree of molecular ordering. Thus the comparison of principal values of ordering can provide information about relative motional amplitudes between segments. The comparison of the magnitude of ordering between segments is often done quantified in terms of a parameter called the

generalized degree of order (GDO), symbolized by ϑ.[64]

$$\vartheta = \sqrt{\frac{2}{3}\sum_{ij} S_{ij}^{\ 2}} \tag{7}$$

The GDO can also be related to the standard deviation of the distribution of RDCs,

$$\sigma_{\mathrm{Dres}} = \sqrt{\frac{1}{5}}\left|\left(\frac{\mu_0}{4\pi}\right)\frac{\gamma_i\gamma_j h}{2\pi^2 r_{ij}^{\ 3}}\right|\vartheta \tag{8}$$

A comparison of GDOs for different molecular domains or segments can provide a lower bound for the extent of motional averaging, as illustrated later in the context of specific applications.

Another regime of interest is when the biomolecule is well-structured yet exhibits motional fluctuations about a mean conformation. From a theoretical point of view, this motional regime can be characterized as one in which the overall molecular alignment remains unaffected by internal motions such that the averaging due to internal motions can be separated from the averaging due to molecular reorientation. It is convenient to specify the Saupe tensor, $\hat{S}$, solely in terms of its five independent elements. These five irreducible tensorial elements can be written as a vector, **s**, and have the following relationship to the elements of the 3×3 Saupe order tensor:

$$\mathbf{s} = \left[S_{zz}, \frac{1}{\sqrt{3}}(S_{xx} - S_{yy}), \frac{2}{\sqrt{3}}S_{xz}, \frac{2}{\sqrt{3}}S_{yz}, \frac{2}{\sqrt{3}}S_{xy}\right] \tag{9}$$

The direction cosine functions, $\cos \alpha_n^{ij}$, describing the molecular geometry in eq 3 can likewise be rearranged into irreducible tensor form, in analogy to the Saupe tensor. The irreducible elements of the residual dipolar tensor, $\hat{R}^{ij}$, for the ijth dipolar interaction can be defined as follows:

$$\mathbf{r}^{ij} = \left[R_{zz}^{ij}, \frac{1}{\sqrt{3}}(R_{xx}^{ij} - R_{yy}^{ij}), \frac{2}{\sqrt{3}}R_{xz}^{ij}, \frac{2}{\sqrt{3}}R_{yz}^{ij}, \frac{2}{\sqrt{3}}R_{xy}^{ij}\right] \tag{10}$$

with

$$R_{kl}^{ij} = \left\langle \frac{1}{2}(3 \cos \alpha_k^{ij} \cos \alpha_l^{ij} - \delta_{kl}) \right\rangle \tag{11}$$

In analogy to the definition of the Saupe order tensor, the angles α_n^{ij} describe the orientation of the ijth internuclear vector relative to the arbitrary reference frame (Figure 1) and the δ_{kl} represent the Kronecker delta function. The angle brackets in eq 11 indicate that the elements of the tensor $\hat{R}^{ij}$ are time averaged due to internal motions. In light of the above definitions, the expression for an RDC observed corresponding to a pair of nuclei i and j becomes

$$D_{ij}^{\mathrm{res}} = -\left(\frac{\mu_0}{4\pi}\right)\frac{\gamma_i\gamma_j h}{2\pi^2 r_{ij}^{\ 3}}\sum_k r_k^{ij} s_k \tag{12}$$

We reiterate that the applicability of this expression rests on the validity of the assumption that internal motions are uncorrelated with overall molecular alignment. Nonetheless, the explicit separation of the effects of internal motion and overall alignment according to eq 12 is desirable because it states the problem as a linear algebraic system of equations for which powerful mathematical methods can be brought to bear, as will be illustrated in section 4. It is worth noting that the irreducible tensorial representations just described are closely related to a description in terms of second rank spherical harmonics. For example, the Saupe order tensor elements are related to averages of the second rank spherical harmonics according to[35]

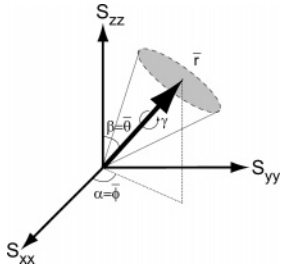

Figure 4. Interpretation of the elements of the residual dipolar tensor in terms of the mean orientation and dynamics of the internuclear vector. The Euler angles (α, β, and γ) describing the transformation that diagonalizes the residual dipolar tensor will specify the mean internuclear vector orientation (α and β) and the direction of asymmetry of motional averaging (γ). The principal values resulting from diagonalization will specify the magnitude and degree of asymmetry of the motion, represented here as an ellipse.

$$\frac{2}{\sqrt{3}}S_{xz} = \sqrt{\frac{1}{2}}\sqrt{\frac{4\pi}{5}}(\langle Y_{21}(\Omega(t))\rangle - \langle Y_{2-1}(\Omega(t))\rangle)$$

$$\frac{2}{\sqrt{3}}S_{yz} = i\sqrt{\frac{1}{2}}\sqrt{\frac{4\pi}{5}}(\langle Y_{2-1}(\Omega(t))\rangle + \langle Y_{21}(\Omega(t))\rangle)$$

$$\frac{2}{\sqrt{3}}S_{xy} = i\sqrt{\frac{1}{2}}\sqrt{\frac{4\pi}{5}}(\langle Y_{22}(\Omega(t))\rangle - \langle Y_{2-2}(\Omega(t))\rangle)$$

$$\frac{1}{\sqrt{3}}(S_{xx} - S_{yy}) = \sqrt{\frac{1}{2}}\sqrt{\frac{4\pi}{5}}(\langle Y_{22}(\Omega(t))\rangle + \langle Y_{2-2}(\Omega(t))\rangle)$$

$$S_{zz} = \sqrt{\frac{4\pi}{5}}\langle Y_{20}(\Omega(t))\rangle \tag{13}$$

in which the spherical angles $\Omega(t)$ describe the orientation of the magnetic field relative to the molecular frame. An analogous expression can be written relating the residual dipolar tensorial elements to the averages of second rank spherical harmonics, which depend on the spherical angles describing the internuclear vector orientation relative to the same molecular coordinate axes.

In the above formulation, the internal and external degrees of freedom have been partitioned into the Saupe and individual residual dipolar tensors corresponding to each dipolar interaction. As discussed, the Saupe order (alignment) tensor can be related to a physical description of molecular alignment. It remains to develop the interpretion of the residual dipolar tensor for a specific dipolar interaction. Due to the symmetry of the formulation described in eqs 9−12, one would expect that this interpretation closely mirrors that of the Saupe tensor. Indeed, a diagonalization of the 3×3 Cartesian matrix representation of the ijth residual dipolar tensor $\hat{R}^{ij}$ does provide the desired physical description.[65,66] This separation into structural and dynamic characteristics is illustrated in Figure 4. If the unitary transformation that diagonalizes $\hat{R}^{ij}$ is parametrized in terms of Euler angles (α, β, γ), then the angles α and β will correspond to the spherical

angles describing the mean orientation $(\bar{\theta},\bar{\phi})$ of the *ij*th internuclear vector. The eigenvalues of $\hat{R}^{ij}$ correspond to order parameters describing the amplitude of motion with the principal value $\hat{R}^{ij}_{zz}$ corresponding to the axial order parameter and the difference $(\hat{R}^{ij}_{xx} - \hat{R}^{ij}_{yy})$ reflecting the asymmetry of motion. The direction of motional asymmetry is described by the third Euler angle, γ. A dipolar generalized order parameter, $\mathbf{S}_{rdc}$, can be related to the principal values of $\hat{R}^{ij}$ according to

$$S_{ij,rdc}{}^2 = [R^{ij}_{zz}]^2 + \frac{1}{3}[R^{ij}_{xx} - R^{ij}_{yy}]^2 \qquad (14)$$

The dipolar generalized order parameter is identical to the generalized order parameter obtained from heteronuclear spin relaxation studies but is sensitive to a much broader motional time scale (picoseconds−milliseconds).

3. Molecular Alignment

Parameters such as dipolar couplings, chemical shift anisotropies, or quadrupolar couplings are not normally observed in solution state NMR spectra because they average to zero under isotropic solution conditions. Thus a prerequisite to the observation of RDCs or other anisotropic parameters is the introduction of an anisotropic solvent environment that is compatible with the biomolecule of interest while still maintaining the conditions necessary for high-resolution NMR. In general, this is accomplished by providing a highly ordered solvent environment, from which a small degree of order is transferred to the solute by means of interactions mediated by the shape or charge distribution of the biomolecule. In this section, we consider different methods for achieving the required molecular ordering as well as techniques for describing the resulting order in a rigorous manner.

3.1. Methods for Inducing Molecular Alignment

The first demonstration of the feasibility of measuring anisotropic parameters such as RDCs in a biomolecule was an application to cyanometmyoglobin (MbCN), in which the molecular alignment was achieved by means of the spontaneous alignment in the magnetic field due to the large paramagnetic susceptibility anisotropy of MbCN.[67] Shortly thereafter, it was shown that liquid crystalline solvents, long used to study small molecules, could be adapted for use in biomolecular applications. The first application using an external alignment medium for biomolecules utilized a mixture of phospholipids, which at specific composition and temperature form an anisotropic phase referred to as bicelles.[68] Because the use of an external medium tends to provide much larger degrees of alignment and is in general applicable to any biomolecule, this stimulated the development of a multitude of ordered media that exhibit compatibility with biomolecules.[12,15−17,26] For convenience, we summarize in Table 1 the media known to be compatible with biomolecules along with their basic characteristics and references to the original work. There are some general considerations for working with the various alignment media. If only one or two sets of RDC data are required, stretched polyacrylamide gels[69−72] or C_nE_m/*n*-hexanol[73] media are good choices for a first attempt due to their high level of compatibility with most biomolecules. For the acquisition of multiple alignment media, the successful acquisition of independent RDC data will likely require the utilization of media that exhibit a variety of different morphologies and electrostatic properties. As a first step, one should consider the desired working temperature and pH and choose those media that are compatible with these conditions. A second consideration should be to consider the net charge of the biomolecule at the working pH. Inevitably, there will be media that carry a charge that is opposite to that of the biomolecule at the working pH. Although this poses the risk of poor spectral quality due to strong interactions with the medium, these media can provide useful complementary RDC data if measures are taken to moderate the strength of the interaction. Specifically, the strength of the interaction can often be moderated by increasing the ionic strength, by reducing the molar concentration of the medium, or if applicable by reducing the molar concentration of the charged species used as a doping agent. An open question is whether stronger interactions with the medium might perturb the structural or dynamic properties of the biomolecule. At present there is little evidence to support this concern, although it is expected that future investigations will shed further light on this question.

3.2. Experimental Determination of the Alignment Tensor

For most RDC applications, the nature of molecular alignment must be established to interpret the RDCs in terms of structural and dynamic parameters. The necessary description of molecular alignment is embodied in five parameters, which make up the alignment (or Saupe order) tensor. In general, the details of molecular alignment are not under tight experimental control, and thus the alignment tensor must be determined from the RDC data and a set of structural coordinates. However there are certain conditions, in particular when alignment is purely steric in nature, under which the alignment tensor can be predicted accurately based on a structure.[74−79] Otherwise, the determination of the alignment tensor proceeds based on a set of structural coordinates and at least five independent RDC measurements. The determination of the alignment tensor amounts to finding the solution to a linear set of algebraic equations. This can be seen by rewriting eq 12 in the following form:

$$\tilde{D}^{res}_{ij} = \frac{D^{res}_{ij}}{K} = [\mathbf{r}^{ij}]^{tr}\mathbf{s}; \quad K = -\left(\frac{\mu_0}{4\pi}\right)\frac{\gamma_i\gamma_j h}{2\pi^2 r_{ij}{}^3} \qquad (15)$$

where the column vector **s** contains the elements of the alignment (order) tensor to be determined and $[\mathbf{r}^{ij}]^{tr}$ denotes the transposed (i.e., row) vector containing the elements of the residual dipolar tensor for the *ij*th dipolar interaction. If multiple RDC measurements are available, then additional row vectors, $[\mathbf{r}^{ij}]^{tr}$, and their corresponding RDC measurements, D_{ij}, can be organized as a set of linear equations,

$$\tilde{\mathbf{d}} = \mathbf{Rs} \qquad (16)$$

in which **d** is a column vector containing the experimental RDC data divided by the interaction constant *K* and **R** is a matrix containing the individual vectors $\mathbf{r}^{ij}$ along its rows. The order tensor **s** is the unknown five dimensional vector to be solved for. As long as at least five independent RDC measurements are available then the five unknown elements

Table 1. Media Employed for the Alignment of Biomolecules

media type	composition	charge	temp (°C)	features	ref
bicelle (ester)	DMPC/DHPC	neutral	30−45	prone to hydrolysis	68,136
	DMPC/DHPC/CTAB	positive	30−45	less prone to hydrolysis	137
	DMPC/DHPC/SDS	negative	30−45	less prone to hydrolysis	137
	DLPC/CHAPSO	neutral	7−50	low temperature	138
bicelle (ether)	DIODPC/DIOHPC	neutral	30−45	pH 1−12, expensive	139
	DIODPC/CHAPSO	neutral	10−60	pH 1−6.5, expensive	140
suspensions of virus particles	bacteriophage Pf1	negative	14−45	pH > 5, aggregates at high ionic strength, sample is recoverable	141,142
	bacteriophage fd	negative	5−60	as above	143,144
	tobacco mosaic virus	negative	5−60	as above	143
purple membrane fragments	2D crystalline fragments of lipids and bacteriorhodopsin	negative	0−70	sample is recoverable; strongly interacts with proteins	145,146
	PM doped with Tb^{3+}	negative	0−70	aligns with normal perpendicular to B_0; reduced line broadening	147
cellulose	cellulose fibers	slightly negative		wide pH range	148
lamellar liquid crystalline phases	C_mE_n/*n*-hexanol	neutral	0−40	inexpensive, insensitive to pH, low binding affinity for biomolecules	73
	C_mE_n/*n*-hexanol/CTAB	positive			149
	cetylPrBr/*n*-hexanol/NaBr	positive	15−60	difficult to prepare, low ionic strength	150,151
	cetylPrCl/*n*-hexanol/NaCl	positive	0−70	high ionic strength	152
paramagnetic field alignment	lanthanide ion replacement			nonperturbing isotropic solution environment, line broadening in proximity to lanthanide ion	153,154
	addition of lanthanide-binding EF-hand			as above	155
	engineered terminal lanthanide-binding tag			as above	156
stretched/ compressed hydrogels	polyacrylamide	neutral	at least 5−45	easy sample recovery, high compatibility with biomolecules, inhomogeneous line broadening	69−72
	polyacrylamide/acrylate	negative		strong osmotic swelling forces complicate preparation	157
	polyacrylamide/AMPS	negative		as above	85
	polyacrylamide/DADMAC	positive		as above	85
immobilized media	polyacrylamide gel/phage Pf1	negative		variable director of ordering	158
	polyacrylamide gel/PM fragments	negative		as above	70
	pluronic F-127/bacteriophage Pf1	negative	20−35	variable director of ordering, reversible, temperature activated	159

of the order tensor can be solved for utilizing the Moore−Penrose (M−P) generalized inverse, $\mathbf{R}^+$,[80−82] of the matrix **R**

$$\mathbf{s} = \mathbf{R}^+\tilde{\mathbf{d}} \quad (17)$$

The M−P generalized inverse of a matrix is easily found based on a singular value decomposition (SVD) of the matrix to be inverted. Losonczi et al. have described in detail the procedure for determining the alignment tensor by means of SVD.[83]

Because the SVD of a matrix has additional applications to the analysis of RDCs, we briefly summarize the relevant aspects here. All matrices can be factored into a product of three matrices via SVD,[80]

$$[\mathbf{M}(k \times l)] = [\mathbf{U}_M(k \times r)][\mathbf{W}_M(r \times r)][\mathbf{V}_M^{tr}(r \times l)] \quad (18)$$

where **U** and **V** are orthogonal matrices and **W** is diagonal and comprised of the singular values. In the context of the determination of alignment tensors from RDCs, the singular values represent an important indicator of the degree to which the internuclear vectors are independent. For this reason, the SVD approach is strongly advantageous relative to nonlinear least squares minimization or grid search approaches, which do not provide an indication as to whether the problem is sufficiently well-determined such that a solution can reliably be obtained. A simple metric for specifying the degree to which the measurements are independent is the condition number,[80−82] defined as the ratio of the largest to smallest singular values, (w_1/w_n). A condition of 1 corresponds to the case in which the measurements are perfectly independent. A poorer distribution of internuclear vector orientations will produce larger condition numbers and correspondingly greater imprecision of estimation of the alignment tensor. Analogously, an SVD analysis provides the means by which the independence of RDC datasets collected in multiple alignment media, as discussed below.

3.3. Assessing the Independence of RDC Data Acquired in Multiple Alignment Media

It is not yet possible to experimentally control the specific details of the alignment of a biomolecule in a given alignment medium. As a consequence, the acquisition of independent RDC datasets using multiple alignment media remains an unpredictable enterprise. Furthermore, the RDC data measured using a different alignment medium will almost certainly not be fully independent of other datasets. So the specification that the RDC data be collected in some specific number of independent media, which is often stated in studies that require a large number of independent datasets, cannot refer to the number of actual samples prepared and placed in the magnet for acquisition of RDC data. Rather, this

specification refers to the number of linearly independent datasets, which are collectively represented by the data. Thus, an important aspect is the means by which the independence of the RDC data is evaluated. For RDCs collected in just two different media, the degree of independence of the RDC data can be accurately reflected by a correlation plot of the two respective measurements or by the tensorial dot product of the associated alignment tensors.[84] For more than two media, while it is possible to establish the nonindependence of the data using these methods, it is not possible to establish the independence of the data. This is because the third, or higher, datasets could simply be linear combinations of the first two. While this might produce a different alignment tensor and different RDCs, it remains possible that there would be no novel information content.

The independence of three or more RDC datasets can be assessed by means of singular value decomposition (SVD). An SVD analysis will reveal the extent to which the datasets are simply linear combinations of one another.[65] As an example, shown in Figure 5 are plots of the singular values of multiple-alignment datasets acquired for the protein ubiquitin and protein GB3. In the case of ubiquitin, 11 distinct datasets have been analyzed, and the singular values indicate that five independent RDC datasets are present.[66] On the other hand, although five distinct alignment media were employed for the measurement of RDCs for protein GB3,[85] the SVD analysis indicates that the data represent strong contributions from only three independent alignments. There is evidence of a fourth independent set, but it is of small magnitude. The difficulty in making this determination based on the magnitudes of the singular values is that one needs to distinguish signal from noise. This is normally achieved by recognizing that random noise will contribute a constant magnitude to the singular values. However, if a set of structural coordinates is available, then these coordinates can be used as an aid to distinguish real signal from noise for a given singular value. This discrimination can be facilitated using the *Q*-value normally used to assess the agreement between a set of measured RDCs and those back-calculated based on a structure. As an aid to analysis, the singular values in Figure 5 have been annotated with their corresponding *Q*-values.

Assuming that no systematic errors are present in the data and that the structure and dynamics of the molecule are not perturbed by one or more of the media employed, there cannot be more than five linearly independent combinations of the measured RDCs that relate to the structural and dynamic properties of the molecule. Therefore, an SVD analysis as described above provides a mechanism by which systematic errors or differences in structure and dynamics between media might be detected. Although formulated in a different manner, this has been described in detail by Hus et al.[86,87] Their approach, dubbed SECONDA, interrogates a set of RDC data collected in multiple alignment media for inconsistencies that might arise due to systematic errors or conformational heterogeneity between media. Furthermore, the SECONDA analysis allows the discrepancies between media to be localized to specific residues. This is a useful aid to the analysis of multialignment RDC data. In employment of this protocol, however, it is important to ensure that a sufficient number of RDC datasets be included to protect against the misinterpretation of systematic errors as real signal.

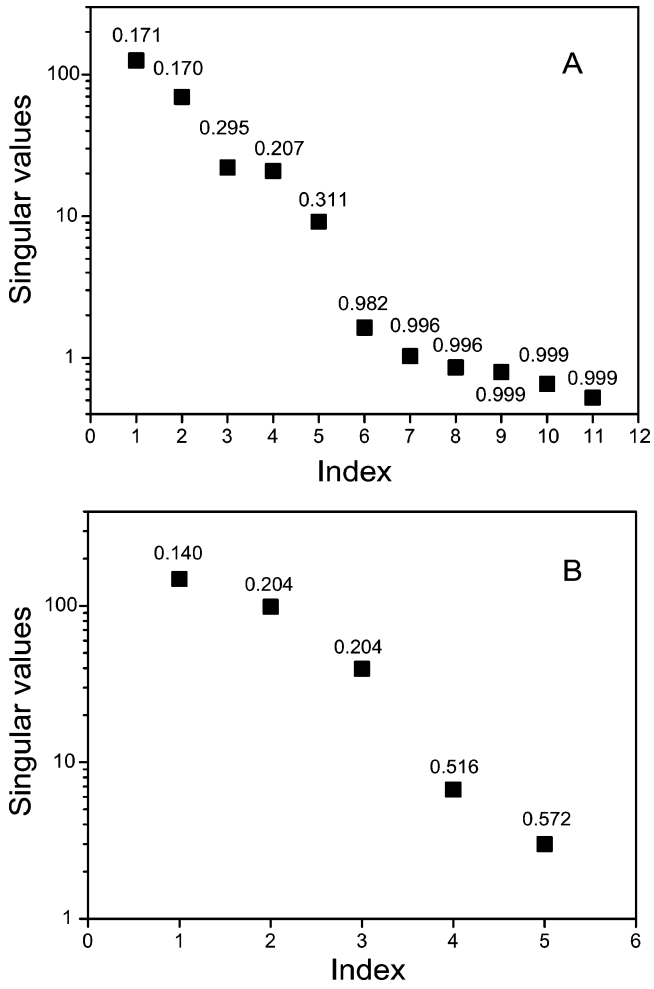

Figure 5. The independence of RDC data acquired in multiple alignment media is assessed by means of a singular value decomposition (SVD) of the data: (A) SVD analysis of 11 datasets acquired for the protein ubiquitin;[66] (B) SVD analysis of 5 datasets acquired for protein GB3.[85] The magnitudes of the singular values reflect the relative contribution of distinct orthogonal linear combinations of the measured couplings within the data. Generally, the number of singular values of relatively large amplitude will correspond to the number of independent datasets contained within the RDC data. However, this interpretation can be complicated if sizable systematic errors are present. Therefore, if a set of structural coordinates is available, it is helpful to compute the *Q*-values that correspond to each singular value. Higher *Q*-values correspond to increasing noise content, with a *Q*-value of 1 indicating random noise.

4. Biomolecular Dynamics from Residual Dipolar Couplings

Measured RDCs report on a time or ensemble weighted average over all conformations assumed by a biomolecule over the course of picoseconds to milliseconds. No specific resolution of the time scales on which these conformational fluctuations occur is carried by the observed RDCs. In a sense, therefore, the development of tools for the study of dynamics from RDCs has been motivated by the observation that a measured set of RDCs is incompatible with the existence of a single molecular conformation. Indeed, deviations from expectations based on a single rigid molecule were first noted in an early application to field-aligned cyanometmyoglobin,[88] prompting the interpretation of the RDC data in terms of rigid helical motions. This interpretation generated considerable controversy at the time,[89] which

persists to some degree at present. This is because the characterization of dynamics by RDCs still predominantly proceeds based on deviations from expectations for a rigid structure. This tension between interpretations of the RDC data in terms of rigid structure or dynamics in general requires that a substantial number of RDC measurements are made to confidently exclude interpretations in terms of a single molecular conformation. Due to the data intensive nature of RDC-based studies of dynamics, applications can be broadly partitioned into two categories: (1) applications in which the analysis is assisted by assuming that domains or local segments of the biomolecule are rigid, thus simplifying the RDC analysis and yet providing for the characterization of motional fluctuations between these rigid elements; (2) applications that make use of extensive sets of RDCs measured under different aligning conditions. We discuss below the different approaches that have been demonstrated to date.

4.1. Domain Motions

It is often the case that individual domains or secondary structural elements can reasonably be assumed to be rigid, and the relative orientation and mobility of domains can be characterized on the basis of an analysis of the ordering experienced by each individual element relative to the magnetic field. The general approach is illustrated in Figure 6. Specifically, the determination of separate order tensors for each domain or fragment allows the mean relative orientation to be established according to the orientation of the ordering PAS and the relative mobility to be established according to the differences in magnitudes of the principal values. The determination of an individual order tensor for each fragment requires that at least five independent RDCs be measured per fragment, although in practice more are desirable to improve the precision to which the order tensor elements can be determined.

An early observation of the effects of motional averaging on measured RDCs was reported for a study of $^1D_{NH}$ RDCs in field-aligned cyanometmyoglobin.[88] It was noted that deviations between measured RDCs and those back-calculated based on solid-state structural coordinates and the paramagnetic susceptibility anisotropy determined from pseudocontact shifts showed systematic departures, which

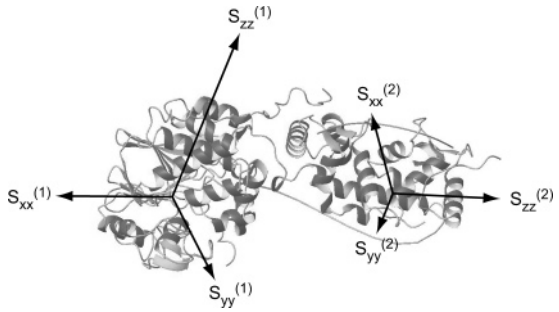

Figure 6. The relative mean orientation and dynamics of two domains can be characterized by the separate determination of the order tensors for each domain. For rigidly connected domains, the determined order tensors should be identical. The mean relative orientation is determined by rotation of the domains such that their principal axes of order coincide. A comparison of the principal values of ordering, indicated by the lengths of the principal axes, provide a measure of relative mobility. Smaller magnitudes of ordering will correspond to greater relative mobility of the corresponding domain.

were correlated within individual helices. It was shown that improved agreement could be obtained if simple rigid helical motions within a cone or along a one-dimensional arc were incorporated into the model. A couple of years later, during a structural study of the B and C domains of barley lectin,[90] it was noted that the magnitudes of RDCs measured for each of the two domains were strikingly different. The authors attributed this to the preferential association of the B domain with the CTAB-doped bicelles used to establish alignment. By employing a bicelle preparation doped with a higher mole fraction of CTAB, the apparent discrepancy in the ordering of the two domains was reduced. The observation of differential ordering between domains was interpreted as evidence of extensive interdomain mobility, on the order of $\pm 40°$ if a cone model is used.

In general the ability to deduce the extent of motions between domains may depend on the ability to align one domain more strongly than the other. This is because large scale domain motions will tend to change the overall alignment in a way that will tend to counteract the effects of averaging.[58,91,92] It follows that the failure to observe a difference in ordering of two domains is not sufficient evidence to conclude that they behave as a single rigid unit. However, given the number of different alignment media now available, for nonequivalent domains it appears unlikely that each domain would interact in the same way with all media. A number of studies have now been reported in which different magnitudes of alignment have been observed for two different domains, implicating dynamics. As pointed out by Braddock et al., these sorts of investigations do not necessarily require that the structure of the domains be known beforehand.[93] Based on an analysis of the distribution of RDCs[94] measured for each of the domains, one can establish the magnitude of alignment for each domain separately and thus identify rapidly cases in which the domains are mobile relative to one another and interact differently with the alignment medium. They investigated two different systems using bacteriophage Pf1 particles to achieve alignment in both cases. The first system was a complex between the KH3 and KH4 domains of the FUSE binding protein (FBP) bound to a 29-base single-stranded DNA from FUSE, and the second system was composed of the N- and C-terminal LEM domains from LAP2.[93,95] Although in both studies the two domains were separated by rather long linkers, it was not evident beforehand whether the two domains interacted strongly with one another. However in both cases the RDCs measured for one domain were twice the magnitude of those measured for the other, indicating the existence of large amplitude interdomain motions. Jacobs et al. have investigated the effects of peptide binding on the peptidyl-proline isomerase Pin1, which is composed of a catalytic domain and a much smaller WW domain attached by a flexible linker.[96] In combination with heteronuclear spin relaxation studies, they employed RDCs measured in two different alignment media to characterize the extent of interaction between the domains. Remarkably, they found that addition of peptide promotes a strong interaction between the otherwise weakly interacting domains. This conclusion was based on the observation of a dramatic increase in the magnitude of WW domain alignment, from a much smaller value to a degree comparable with the catalytic domain upon peptide binding. There have other applications in which more modest amplitudes of interdomain dynamics were detected, including the study of the peptide-bound SH2 and SH3

domains of FynSH32[97] and the two domain protein SP14.3 from *Streptococcus pneumoniae*.[98]

It is not always possible to unambiguously establish from the RDC data the existence of a dynamic equilibrium between different domain orientations in solution as opposed to a single static conformation of the domains that differs from that observed in solid state or solution state structures determined under different conditions. This ambiguity can often be lifted by additional experimental information, in which case the RDCs can provide powerful structural restraints on the nature of the static rearrangement or the distinct conformations in dynamic equilibrium. There are now a number of studies that illustrate this approach. Lukin et al. have used RDC measurements, employing two different alignment media, to study the quaternary structure of carbonmonoxy-hemoglobin (Hb).[99] They conclude that Hb exists in solution as a dynamic intermediate between the R and R2 states, which have been determined by crystallographic methods. A dynamic model of Hb is further supported by the observation of chemical exchange broadened resonances at the interface affected by the R to R2 transition. Using an array of techniques including RDCs and ^{15}N spin relaxation approaches, Varadan et al. have found that the ubiquitin subunits in polyubiquitin chains exhibit flexibility relative to one another at neutral pH but not at lower pH.[100] Goto et al. have investigated the solution state conformation of bacteriophage T4 lysozyme based on extensive RDC measurements and proposed that it exists in dynamic equilibrium between "open" and "closed" conformations.[101] The same laboratory has also carried out an intricate set of studies on the conformation of maltodextrin-binding protein (MBP) in its apo, maltodextrin-bound, and maltotriose-bound forms.[91,102]

An interesting set of studies have been carried out by Al-Hashimi and co-workers, which illustrates nicely the use of RDCs for the characterization of the tertiary structural dynamics in nucleic acids. These investigations have centered around the transactivation response element (TAR) RNA from HIV-1 using bacteriophage Pf1 as an alignment medium. The interaction of TAR with the protein Tat is important for viral replication, and thus it is of interest to understand its conformational properties. In their earliest report, they demonstrated that TAR, in the absence of divalent cations, assumes on average a bent conformation with an interstem angle of approximately 46° while undergoing large amplitude fluctuations about this average on the order of $\pm 47°$.[103] Based on these results, they concluded that Tat recognizes TAR by means of a tertiary capture mechanism. Subsequent studies looked at the conformation of TAR in the presence of Mg^{2+}, argininamide, and the molecules neomycin B and acetylpromazine. It was shown that both argininamide and Mg^{2+} lead to quenching of interstem motions in TAR and a nearly collinear arrangement of the stems.[104] Furthermore, argininamide led to formation of additional hydrogen bonding interactions in the bulge region. Binding of the highly charged neomycin B also produced a quenching of TAR motions, while acetylpromazine, which carries only a single charge, led to only a modest reduction in the TAR interstem mobility.[105]

As we have mentioned, one of the difficulties associated with studies of dynamics of two domains is that the effects of motions on the observed RDCs can be masked in part due to changes in the molecular alignment that correlate with the instantaneous conformation. Skrynnikov et al. have pointed out that for the case of two equivalent domains, the effects of motions may become completely transparent due to this correlation effect.[91] In the absence of preferential association of one of the domains with the alignment medium, one approach to overcoming this potential limitation is to utilize field-induced orientation rather than an external aligning medium. A recent demonstration of this approach introduced paramagnetic field induction of just one of the domains of calmodulin (CaM).[106] Building on some previous RDC-based structural studies on CaM,[107] they have measured pseudocontact shifts (PCSs) and RDCs by modification of the N-terminal domain to preferentially bind lanthanide ions. Striking differences in magnitude of RDCs measured for each domain were observed, indicating substantial mobility between the domains. They undertook a search of sterically allowed combinations of CaM conformations, which produced averaged PCSs and RDCs that were consistent with observation. They found that a uniform sampling over all conformations did not reproduce the data well. Better agreement was found using a model in which, relative to a fixed N-terminal domain, the C-terminal domain moves within a wide elliptical cone with a clearly defined spatial disposition relative to the N-terminal domain.

Field-induced alignment studies are also feasible for nucleic acids, which typically assume conformations in which the aromatic bases are stacked, leading to sizable diamagnetic susceptibility anisotropies. Zhang et al. have proposed an approach in which interstem motions in nucleic acids can be characterized by means of comparison of the experimentally measured $\Delta\chi$, which is determined from the RDC data, and a calculated $\Delta\chi_{calcd}$ derived from tensor summation of the individual base magnetic anisotropies.[92] They found even larger amplitudes of interstem motion for TAR than in the Pf1-based study discussed above. A similar approach was applied to the determination of the global structure in solution of the Holliday junction.[108] Using a sparse set of RDCs, the authors demonstrated that the global conformation of this branched nucleic acid molecule could be established on the basis of the requirement that agreement be reached between the experimental $\Delta\chi$ derived from the RDC measurements and the predicted $\Delta\chi$ calculated by a structure-based tensorial summation of individual base anisotropies. The residual discrepancy between the calculated and experimentally derived $\Delta\chi$ was consistent with interhelix motions with approximately a 28° cone semiangle. The precision with which amplitudes of motion can be determined by this approach has been recently questioned utilizing a DFT/GIAO calculation of individual base anisotropies combined with an RDC−NMR study of the Dickerson dodecamer.[109] An accurate knowledge of base anisotropies is necessary for the interpretation of field-induced RDCs in terms of nucleic acid dynamics. The authors found that their experimental RDC data and the results of calculation were in excellent agreement and consistent with substantially smaller base anisotropies than have been typically utilized.

4.2. Local or Segmental Motions

An approach similar to that employed to probe the motions of domains can likewise be applied to smaller fragments of a molecule. In an application to ubiquitin, individual peptide planes and their adjacent C^{α} moieties were treated as rigid subunits, and then a comparison of the fragment-specific GDOs determined from an extensive set of RDCs in a single alignment medium was used to probe the amplitudes of

motional fluctuations along the peptide backbone.[64] A related approach has been applied to a fragment of *Escherichia coli* 23S ribosomal RNA.[110] In this study, five different RDC measurements were made per ribose unit based on single 3D experiment. From these data, axial and rhombic magnitudes of alignment were determined for individual ribose units, employing a restrained order tensor calculation in which the magnitudes were grid-searched while the orientations were fit. Evidence for mobility was found for a terminal residue by comparison against the order tensor calculated for the entire stem using an idealized A-form geometry. A challenge is to obtain enough measurements to achieve an acceptable precision of determination of the magnitudes of alignment.[111] Acquisition of RDC data in two different alignment media is one route by which this difficulty can be mediated. An alternative method for improving the precision of determination of the magnitudes of alignment for small peptide fragments has been proposed by Bryce and Bax. In the extended histogram method (EHM),[112] measured RDCs corresponding to an individual planar peptide bond unit are supplemented with additional synthetic couplings calculated by utilizing the known geometrical relationships between the corresponding bonds of the peptide plane unit. Particularly significant is the ability to calculate a synthetic RDC corresponding to the peptide plane normal.

Even in cases where fewer RDC data are available, RDCs can be used as probes of localized flexibility to complement other NMR probes of dynamics. In an application to ribonuclease binase, Zuiderweg and co-workers determined order tensors from one-bond amide N−H RDCs for contiguous five-residue segments along the protein backbone.[113] With a couple of exceptions, regions that showed departures in the order tensor magnitudes or principal axis frames corresponded to regions that were identified as undergoing slow conformational motions by means of ^{15}N R_2 measurements. A similar approach has been applied to a study of a complex between the catalytic domain of stromelysin (MMP-3) and the tissue inhibitor of metalloproteinases 1 (TIMP-1).[114] In a structure determination of micelle-bound α-synuclein using molecular fragment replacement (MFR),[115] Ulmer et al. found that the alignment magnitudes obtained for the seven-residue fragments used to build the MFR model exhibited very large differences along the backbone.[116] Remarkably, this RDC-based analysis revealed extensive dynamics not picked up by an accompanying ^{15}N spin relaxation analysis. The authors concluded that there must be rigid helical motions that are occurring on the microsecond time scale. If the amplitudes of localized motions are particularly pronounced, these regions may be illuminated by the observation of striking deviations of specific measured RDCs from predictions based on a structure. Such effects have been reported in an application to a destabilized mutant of protein GB3[117] and the catalytic domain of matrix metalloproteinase 12.[118]

4.3. Generalized Order Parameters from Residual Dipolar Couplings

A widespread technique for the analysis of heteronuclear spin relaxation data is the so-called "Lipari−Szabo" model-free formalism,[119] which provides a set of correlation times describing the motional time scale and an order parameter related to the amplitude of orientational fluctuations of each individual internuclear vector. Formally, the generalized order parameter refers to the average value over a sum of squared

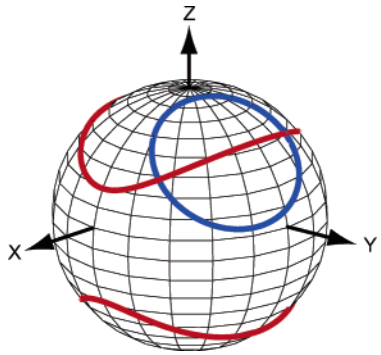

Figure 7. Acquisition of RDC data in a second *independent* aligning media allows the possible internuclear vector orientations to be reduced to a discrete number of possibilities indicated by the intersections between different cones.

second rank spherical harmonic functions describing the time-dependent orientation (θ(t), ϕ(t)) of the internuclear vector relative to a fixed molecular frame,

$$S^2 = \frac{4\pi}{5}\sum_{m=-2}^{2}\langle Y_{2m}^{*}(\theta(t),\phi(t))\rangle\langle Y_{2m}(\theta(t),\phi(t))\rangle \quad (19)$$

Reorientation of the whole molecule serves to erase the effects of internal motional averaging of internuclear vectors and thus the information about motional amplitude contained in the spin relaxation derived generalized order parameter squared is restricted to time scales faster than the correlation time of the whole molecule (nanoseconds for proteins in solution). Residual dipolar couplings depend on the same spherical harmonics with sensitivity proportional to the generalized order parameter S rather than the S^2 dependence for spin relaxation, yet they persist through the NMR time scale of observation (generally milliseconds). Thus, RDCs represent a probe by which generalized order parameters can be determined over a broad time scale spanning picoseconds to milliseconds. The difficulty is that while several relaxation rates can be measured for a given nuclear spin pair, only one RDC measurement can be made for each internuclear spin pair for a given aligned sample. This can be overcome by the measurement of complementary RDCs using samples in which the molecular alignment is varied by use of different aligning media. Although this approach is experimentally demanding, it has now been demonstrated that sufficient RDC data can be interpreted in terms of generalized order parameters, including a description of the direction and degree of asymmetry of motional averaging.

To understand how such detailed information about dynamics may be extracted from a set of RDCs acquired under different aligning conditions, it is instructive to consider the nature of the information contained in a measured RDC. A single RDC will correspond to a continuum of possible internuclear vector orientations relative to the principal axis system (PAS) of alignment, with these solutions appearing as a flattened cone when plotted on the surface of a sphere (Figure 3). It is common to lift this ambiguity by acquisition of RDCs in a second *independent* aligning media, thus producing an additional, different cone of possible orientations.[120,121] This will restrict the possible internuclear vector orientations to just a discrete number (typically four) of possibilities, as shown in Figure 7. If a third alignment medium is employed, linearly independent of the first two, then it is clear that a unique solution (except

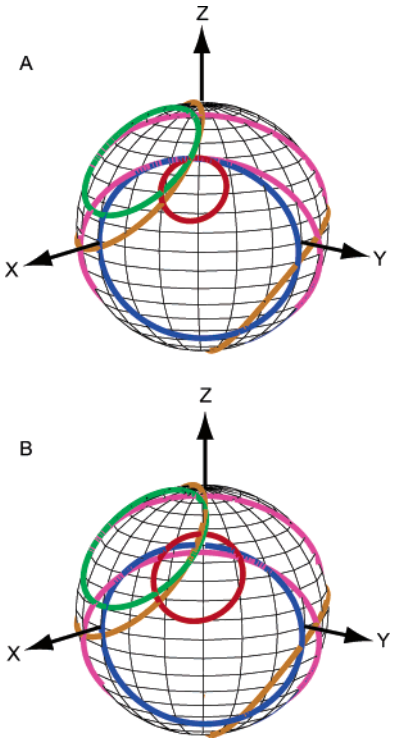

Figure 8. Acquisition of RDC data in five independent alignment media can unambiguously establish the orientation of a single internuclear vector and provide information about dynamics: (A) For a rigid internuclear vector, all five cones will coincide and the orientation will be overdetermined; (B) For a dynamic internuclear vector there will not necessarily be a common intersection. This provides a route by which the dynamics can be characterized. Shown are the resulting cones for case of relatively modest motional amplitude ($S = 0.9$ and asymmetry $\eta = 0.044$).

for inversion) will be obtained. Subsequent acquisition of a fourth or fifth independent RDC dataset will produce an overdetermined situation for a rigid molecule, allowing for the refinement of the local geometry to a high level of precision.[85] However, if the internuclear vector is undergoing internal motion, then the averaging of the corresponding RDC in each of the media will be different and the cones will no longer intersect. This is illustrated in Figure 8 for a rigid internuclear vector and for one that is dynamic. Because of the very specific dependence of the averaging of RDCs on the spatial nature of the motions, detailed information about internuclear vector motions can be obtained by requiring that all of the motionally corrected cones have a common intersection. Two different formalisms for the determination of generalized order parameters from RDCs measured in multiple alignment media have been introduced.

The first of these approaches was introduced by the Griesinger laboratory[122,123] and is referred to as the model-free approach in recognition of the generalized order parameters obtained from heteronuclear spin relaxation analysis using the Lipari−Szabo formalism. The rationale underlying their approach is that just as five independent RDC measurements along with knowledge of the molecular structure can allow the alignment tensor to be determined, the acquisition of RDCs in five independent alignment media can allow the five independent elements of the residual dipolar tensor for each internuclear vector to be determined. The elements of the residual dipolar tensor for a given internuclear vector can be specified in terms of averages over the second rank spherical harmonics, $\langle Y_{2m}(\theta^{mol},\phi^{mol})\rangle$, which are functions of the spherical angles $(\theta^{mol},\phi^{mol})$ describing the orientation the internuclear vector relative to the alignment PAS. These averages are closely related to those introduced in section 2 (eqs 10, 11, and 13). While for a rigid internuclear vector these five spherical harmonics will depend only on the angular parameters θ^{mol} and ϕ^{mol}, dynamic averaging will cause each of these averages to assume a value that encodes information about the vector orientation and dynamics. If these five averages can be measured, then it is straightforward to recast them into a mean internuclear vector orientation and three dynamic parameters describing the extent of motional averaging (i.e., the generalized order parameter), and the degree and direction of asymmetry of motion.[122]

In practice, the model-free approach proceeds by measurement of RDCs using many different alignment media, followed by calculation of the corresponding alignment tensors based on a set of structural coordinates. The irreducible tensorial descriptions of each of the alignment tensors are arranged into the so-called **F** matrix. This matrix is of dimension $5 \times M$, where M is the total number of RDC datasets acquired. The requirement is that five independent alignment tensors are obtained with sufficient sampling such that the matrix **F** is nonsingular. As discussed in section 3, this can be assessed by consideration of the condition number, which is obtained by taking the ratio of largest to smallest singular values of the matrix **F**. The authors recommend that the condition number be less than 10 to ensure adequate precision of the determined parameters.[123] If this requirement can be experimentally fulfilled, then the individual residual dipolar tensors, represented here by the averages $\langle Y_{2m}(\theta^{mol},\phi^{mol})\rangle$, can be determined by means of a linear algebraic solution to the set of linear equations based on the inversion of the matrix **F**. The set of linear equations can be constructed according to

$$\frac{D_i^{exp}}{D_{i,zz}} = \sum_{m=-2}^{2} F_{i,m}\langle Y_{2m}(\theta^{mol},\phi^{mol})\rangle \qquad (20)$$

in which D_i^{exp} refers to the experimental dipolar coupling measured for the ith alignment medium. The Y's refer to the five averaged spherical harmonics describing the internuclear vector in the molecular frame and $D_{i,zz}$ refers to the principal magnitude of the ith alignment tensor.

Peti et al. have illustrated their model-free approach in an application to the protein ubiquitin.[123] Backbone amide N−H RDC measurements were made using 11 different alignment media. They obtained RDC measurements with a sufficiently small condition number for 32 backbone amide N−H sites. They observed relatively large fluctuations in generalized order parameters between sites, with S_{rdc}^2 ranging between 0.5 and 1.0. One of the difficulties associated with RDC-based studies of dynamics is that it is not possible to firmly establish the absolute magnitude of alignment, and thus the magnitude of order parameters is subsequently undetermined by a single scaling factor that is common for all order parameters. The authors suggest this scaling factor might be established on the basis of measurement of $^1H^N-^1H^\alpha$ RDCs, which are expected to be less sensitive to internal motions than the amide $^{15}N-^1H$ RDCs. By this means, they conclude that the magnitude of the alignment tensors determined from $^{15}N-^1H$ RDCs was underestimated by a factor of at least 0.78.

The Griesinger laboratory has extended their analysis of the amide N−H RDCs measured for ubiquitin, focusing on the single α-helix in ubiquitin.[124] They note that for the six residues within the helix for which they have sufficient data, the results from their model-free analysis indicate highly asymmetric motions, which remarkably exhibit very similar principal direction of motional asymmetry. Although RDCs do not directly probe correlated motions, one might infer the existence of correlated motions when parameters describing motional asymmetry are similar for sites that are expected to be part of a rigid secondary structural element. Using molecular mechanics calculations, Meiler et al. showed that the asymmetrical helix motions consistent with their model-free analysis (±22.5°) could exist without violating any of the NOE restraints for ubiquitin by more than 0.2 Å.[124]

Tolman has proposed an alternative method that provides a similar description of generalized order parameters and motional asymmetries but does not require that a structural model be available.[65] This approach bypasses the need for a priori estimation of alignment tensors by optimizing the residual tensorial elements, which contain the desired description of internuclear vector mean orientations and dynamics, in aggregate such that overall motion for the entire molecule is minimized. Formally, this procedure stems from a representation of the multialignment RDC data in its entirety within a single matrix equation,

$$\mathbf{D} = K\mathbf{B}\mathbf{A}; \quad K = -\left(\frac{\mu_0}{4\pi}\right)\frac{\gamma_I\gamma_S h}{2\pi^2 r_{IS}{}^3} \tag{21}$$

The $N \times M$ matrix **D** contains the actual RDC measurements row-indexed by site and column-indexed according to the specific alignment medium. The matrix **B**, which is of dimension $N \times 5$, contains the irreducible residual tensorial components describing each of the N individual dipolar interactions, and the matrix **A** contains the corresponding irreducible tensorial descriptions of the alignment tensors. The irreducible elements of these tensors are defined according to eqs 4, 9, 10, and 11, with the relevant angles illustrated in Figure 1. In common with Griesinger's model-free approach, it is absolutely necessary that RDC measurements be available from five independent alignment media. Indeed, with the notation introduced in eq 21, the model-free approach could be summarized as the solution to

$$\mathbf{B} = \mathbf{D}\mathbf{A}^{+} \tag{22}$$

in which the elements of the matrix **B** can readily be related to the averaged spherical harmonics $\langle Y_{2m}(\theta^{mol},\phi^{mol})\rangle$ and the matrix **A** matrix differs from Griesinger's **F** matrix only in scaling according to the principal magnitude of alignment and the interaction constant K. Tolman's method, referred to as direct interpretation of dipolar couplings (DIDC),[65] proceeds on the basis of recognition that the ranges of the matrices **D** and **B** in eq 21 are identical when five independent alignment media have been employed for the measurement of RDCs. Under these circumstances, the residual tensorial descriptions of each of the individual dipolar interactions (contained in **B**) can be almost completely written in terms of the RDC data, according to

$$\mathbf{B} = \mathbf{U}_D\mathbf{\Lambda} \tag{23}$$

where $\mathbf{U}_D$ is the $N \times 5$ column-orthogonal matrix specifying a basis that spans the range of the data matrix **D** and the matrix $\mathbf{\Lambda}$ is the 5×5 matrix that embodies the remaining unknown parameters. The matrix $\mathbf{U}_D$ can alternatively be thought of as the matrix of the five normalized and orthogonal RDC datasets constructed from linear combination of the actually measured RDC data that constitute the desired five independent sets of RDC data. This is illustrated

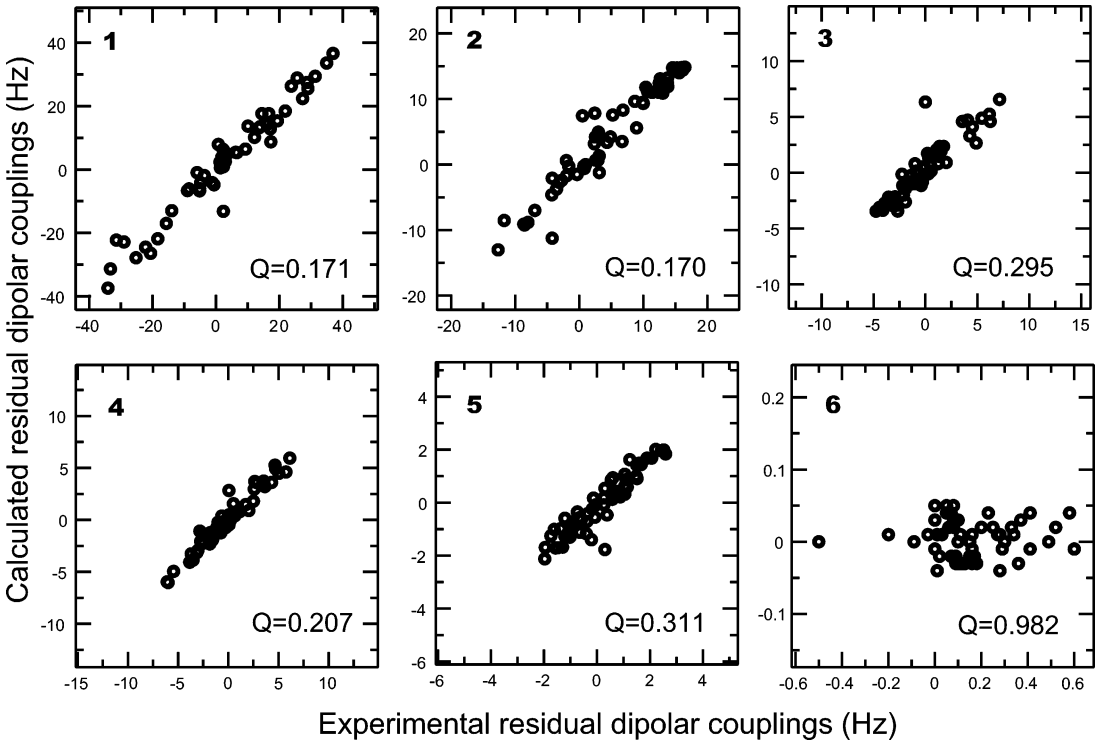

Figure 9. Correlation plots of the five independent linear combinations of experimental RDCs measured for the protein ubiquitin[66] versus the RDCs predicted from the X-ray structure (PDB 1UBQ). For comparison, the sixth experimental linear combination (which corresponds to random noise) is also plotted against predictions based on the X-ray coordinates.

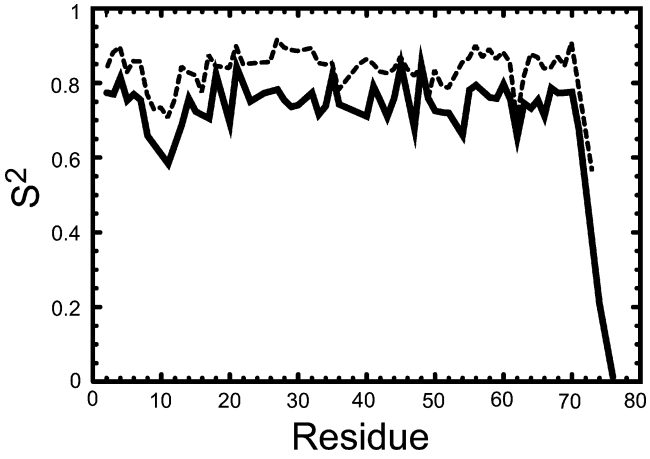

Figure 10. Comparison of generalized order parameters for ubiquitin determined from RDCs (solid line) and from ^{15}N spin relaxation (dashed line). Due to their sensitivity to a broader motional time scale, the dipolar order parameters have been scaled uniformly such that they are smaller than the ^{15}N spin relaxation generalized order parameters.

in Figure 9, which shows these experimental combinations of RDCs scaled to reflect their relative contributions to the data and plotted against the RDCs that are calculated on the basis of the X-ray structural coordinates (PDB 1UBQ[125]). Note that the *Q*-values for each set are all consistent with expectations for a high-resolution solution structure. The magnitudes vary considerably, which reflects that the five independent sets of RDC data are not equally represented in the data. These five RDC basis vectors (i.e., the matrix $\mathbf{U}_D$) were constructed from independent combinations of amide N−H RDC data measured for ubiquitin in 11 different alignment preparations,[66] based on the singular value decomposition of the matrix **D** (which produces $\mathbf{D} = \mathbf{U}_D\mathbf{W}_D\mathbf{V}_D^{tr}$).

The unknown matrix $\mathbf{\Lambda}$ describes proper combinations of these five RDC basis vectors to form the desired residual tensorial elements of each of the internuclear vectors. In the DIDC approach, the matrix $\mathbf{\Lambda}$ is estimated by selecting the solution for $\mathbf{\Lambda}$ that produces the minimum variation in the resulting generalized order parameters.[65] This is achieved by the minimization

$$||\mathrm{Diag}\{\mathbf{U}_D\mathbf{\Lambda}\mathbf{\Lambda}^{tr}\mathbf{U}_D^{tr}\} - \mathbf{1}^{(N)}||_{min} \qquad (24)$$

in which **1** represents the identity matrix. The DIDC approach will produce a set of mean internuclear vector orientations and a description of dynamics that will exactly explain the data. It is important that efforts be made to minimize the entrance of systematic errors into the measurements as well as to ensure that the protein is not substantially perturbed by interaction with the media. As discussed by Brueschweiler and co-workers (see section 3),[86,87] these sorts of problems are detectable on the basis of a knowledgeable assessment of the singular values of the RDC data. An experimental demonstration of the DIDC method was carried out in an application to the amide N−H bonds of ubiquitin.[66] The resulting order parameters, shown Figure 10, show modest site-to-site variability and exhibit a correlation ($r = 0.63$) with ^{15}N spin relaxation order parameters for ubiquitin.[126] These results are consistent with a view of ubiquitin in which motions occurring on slower microsecond to millisecond time scales do not substantially differ in nature from those occurring on the picosecond time scale. Mean N−H bond orientations for ubiquitin, resulting from DIDC analysis, exhibit an agreement with the RDC-refined orientations (starting from either NMR or X-ray structural coordinates) to within 2°, which is close to agreement within experimental precision.

4.4. Peptide Plane Dynamics

It has been observed both by molecular dynamics simulations and by NMR spin relaxation studies that proteins exhibit crankshaft-type wobbling motions of the peptide plane.[127,128] It is likely that these motions constitute an important part of the backbone N−H order parameters derived from ^{15}N spin relaxation studies because the amide N−H bonds are nearly perpendicular to the crankshaft rotation axis and thus are particularly sensitive to these motions. Often, these motions are described in terms of the Gaussian axial fluctuation (GAF) model.[129] In its simplest version (the so-called 1D GAF model), the motional amplitude is described by means of a single parameter, namely, the angular standard deviation characterizing the extent of rotational fluctuations of the peptide plane about an axis joining the C^{α}_{i-1} and C^{α}_{i} atoms. More generally, the 3D GAF model can be employed, which in addition includes single axis rotational motions about the two other orthogonal axes. Results from MD simulations and NMR spin relaxation studies indicate that it is the crankshaft type rotational motions of the peptide plane that exhibit the largest amplitude of fluctuations.[127,128]

Due to the broad time scale sensitivity of RDCs, it is of interest to investigate the nature of these peptide plane motions beyond the picosecond time scale probed by heteronuclear spin relaxation studies. Furthermore, because these motions are known to exist, improvements in the structural interpretation of RDCs might reasonably be achieved if they can be taken into account. Bernado and Blackledge have published a couple of nice papers that establish the means for accounting for and characterizing the extent of such peptide plane motions from RDC data.[59,60] They show convincingly that accounting for these motions leads to improvements in the agreement between experimental RDCs and those back-calculated from a set of structural coordinates. Their approach proceeds from a modification of the equation used to fit measured RDCs to a structure (eq 5).[60]

$$D_{ij}^{o-GAF} = -\left(\frac{\mu_0}{4\pi}\right)\frac{\gamma_i\gamma_j h}{4\pi^2 r_{ij}^3}\left\{\frac{S_{zz}}{4}[s_1(3\cos^2\beta - 1) + 3s_2\sin^2\beta\cos 2\alpha] + \frac{1}{4}\eta\left[s_1\sin^2\beta\cos 2\gamma + 2s_2\left(\cos^4\frac{\beta}{2}\cos 2\delta_1 + \sin^4\frac{\beta}{2}\cos 2\delta_2\right)\right]\right\} \qquad (25)$$

with

$$\delta_1 = \alpha + \gamma; \quad \delta_2 = \alpha - \gamma; \quad s_1 = 1 + 3\,e^{-2\sigma^2}; \quad s_2 = 1 - e^{-2\sigma^2}$$

This expression has been slightly modified for consistency with the theoretical development of section 2. The parameters α, β, and γ are the Euler angles describing the transformation that places the N−H bond vector along the local frame *z*-axis and the peptide plane normal along the *x*-axis. Because these Euler angles can be derived from a structure, the only

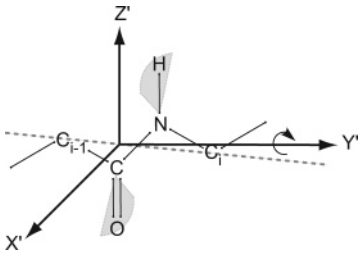

Figure 11. Depiction of the 1D ortho-GAF model for the description of peptide plane crankshaft motions. Based on a set of structural coordinates, each peptide plane is transformed into a local coordinate frame (indicated by the primed axes) such that the N−H bond lies along the z' axis and the peptide plane normal lies along the x' axis. Motional fluctuations are modeled as rotations about the y' axis, which is inclined by approximately 11° from the axis joining the proximal C^{α}_{i-1} and C^{α}_{i} atoms.

additional parameter to be fit is σ, which is the standard deviation of peptide plane fluctuations about the *y*-axis in the local frame (Figure 11). Since the definition of the rotational axis deviates slightly from that of the 1D GAF, the authors call this the ortho-GAF model. With RDCs collected in just a single alignment medium, there are insufficient data for the separate determination of a σ corresponding to each peptide plane; however a common motional amplitude, σ_{av}, can be fit to all peptide planes. Even with this simple approach, for four different proteins (lysozyme, sulfite reductase, dihydrofolate reductase, and methionine sulfoxide reductase), significant improvements in the χ^2 of the fit were found using a common ortho-GAF amplitude.[60] For a fifth protein, ubiquitin, significant improvements were not seen, however the authors attribute this to poor orientational distribution of amide N−H orientations. In support of this conclusion, improvements in the fit using the ortho-GAF model were seen when RDCs in additional alignments were considered. For all proteins examined, the best fit ortho-GAF amplitude σ_{av} ranged between 14° and 17°. Although the utilization of a common ortho-GAF amplitude for all peptide planes contains limited information about dynamics, the authors emphasize that the effects of such highly specific anisotropic motions on RDCs are distinguishable from the effects of errors in coordinates (i.e., structural noise) or motions that are more symmetric in nature. This enables the rapid assessment of average small amplitude peptide plane fluctuations and allows an improved estimate of the order tensor to be obtained, often with substantially improved agreement with the experimentally measured couplings. The improved estimation of alignment tensors enables internuclear vector orientations to be established with higher precision and accuracy.

The inclusion of RDC data collected in a second (or additional) alignment medium can allow ortho-GAF amplitudes to be determined individually for each peptide plane. Bernado and Blackledge have carried this out in applications to protein GB3 and lysozyme.[59] For both proteins, very high-resolution X-ray structures are available along with high-quality sets of RDCs measured in multiple alignment media. For protein GB3, they found ortho-GAF amplitudes mostly on the order of 20°; however, for one loop amplitudes approached 40°. To compare their amplitudes against spin relaxation order parameters, they converted their GAF amplitudes into dipolar order parameters. They found that the dipolar and spin relaxation generalized order parameters were generally correlated yet with nearly all dipolar order parameters being smaller than the spin relaxation order parameters, as expected due to the much broader time scale sensitivity of RDCs. Both sets of order parameters correlated well with expectations based on crystallographic *B*-factors. Likewise, for lysozyme, the dipolar generalized order parameters squared (which were as low as 0.5 in the loops) predominantly exhibited greater motional amplitudes for regions with higher *B*-factors. Because several lysozyme structures are available at different resolutions, the authors explored the consequences of the use of a lower resolution structure on their best fit ortho-GAF amplitudes. They found that although the precision of determination of σ substantially degraded in going from a 0.9 to a 2.1 Å structure, by establishing selection criteria by which solutions for individual peptide planes could be evaluated, they could filter out the low precision GAF amplitudes even when using the 2.1 Å structure.

4.5. Ensemble Simulated Annealing

In the applications discussed thus far, the RDC data have been used either to fit specific models for the motion or to characterize motional amplitudes and asymmetries in a "model-free" manner. For any fit to a motional model, the implicit assumption is that the existence of any unaccounted for motions or structural features will not unacceptably distort the interpretation. In the case of the model-free approaches, there remains the nontrivial undertaking of integrating the site-specific descriptors of the motion into a unified picture of molecular dynamics. In an effort to both avoid explicit dependence on a model and produce an atomic level description of motions, Clore and Schwieters have developed an ensemble simulated annealing approach for refinement of protein structures.[130,131]

The ensemble simulated annealing approach builds on well-established protocols for the determination of solution state structures from NMR spectroscopic data, for the development of which Clore has played a prominent role.[22] The fundamental approach remains unchanged in that high-temperature simulated annealing calculations are carried out in the presence of a potential energy function, which, in addition to the typical force field terms, also contains a number of experimental pseudoenergy terms that serve to produce a molecular conformation that is consistent with all of the NMR data. The distinguishing feature of the ensemble refinement approach is that separate molecular coordinates are refined in parallel, with the agreement between experimental restraints and the instantaneous conformations determined according to the calculation of the relevant averaged NMR parameters over the ensemble. Of course, the ability to refine an ensemble simultaneously requires substantial experimental data, which in this case is provided by extensive RDCs measured in multiple alignment media. To deal with the need for knowledge of alignment tensors, the starting point is not an extended peptide strand but rather the three-dimensional structural coordinates for the protein of interest. This enables the simulated annealing to proceed with both magnitudes and orientations allowed to float.

Clore and Schwieters have demonstrated the approach in applications to two different proteins for which extensive RDC data are available, ubiquitin[130] and the B3 IgG binding domain of streptococcal protein G (GB3).[131] In the application to ubiquitin, a statistically significant yet small improvement in agreement between calculated and experimental RDCs is observed in going from an ensemble size of 1 to 2, although not within the reported experimental precision of

measurement. The authors argue that this discrepancy arises due to a significant underestimate of measurement errors in the original account, based on the comparison of ubiquitin RDCs measured by two different laboratories. Although plausible, this explanation remains inconclusive due to the alternative possibility that the observed differences in RDCs arise from changes in the effective alignment tensor due to likely variations between labs (or even between distinct sample preparations) of such variables as ionic strength or pH. Aside from a few residues that show large amplitude jumps between the two members of the ensemble (S^2(jump) < 0.8), very small deviations were observed for most residues. The two conformers exhibited very small deviations in atomic rms positions, reflecting that jumps between the two members of the ensemble were accompanied by correlated shifts in backbone ϕ and ψ dihedral angles. The results were generally similar for protein GB3, except that the agreement between experimental and calculated RDCs was significantly better for a two member ensemble (relative to one) and was at the level of experimental precision of measurement. Although the motions were again of relatively small amplitude for most residues, it is clear that, if sufficient RDC data are available, is feasible to characterize very subtle anisotropic motions of the peptide backbone.

Another feature of the ensemble simulated annealing approach is that it allows the extent and nature of correlated motions to be discussed. For both ubiquitin and GB3 applications, while no long-range correlated motions were observed, there were extensive local correlated fluctuations consistent with peptide plane crankshaft motions. This fits in well with the results for the study of peptide plane ortho-GAF motions in GB3 carried out by Bernado and Blackledge.[59] For the applications to both ubiquitin and GB3, ensembles larger than two were looked at, but no significant improvement in the agreement between calculated and experimental RDCs was obtained. As the authors note, the ensemble simulated annealing approach provides a model that exhibits the minimum amplitude of motion. There are many models that would exhibit larger motional amplitudes and remain consistent with the RDC data. This is underscored by the observation that the RDC-derived order parameters from the ensemble simulated annealing approach are generally larger than those obtained from spin relaxation methods. This can be understood as a consequence of allowing the alignment tensors to float during the simulation, which will tend to absorb much of the axially symmetric component of the motion into the subsequently reduced magnitudes of alignment. In theory, this is valid; however one must exercise caution in the interpretation of the resulting ensembles because they may exhibit very nonphysical geometries due to the absorption of some of the motion into the tensor magnitudes.

In certain cases, specific models for localized conformational heterogeneity may be introduced that subsequently can be fit to the RDC data. Wu et al. employ this route in the structure determination of a DNA dodecamer utilizing extensive RDC and ^{31}P chemical shift anisotropy (CSA) data.[132] In particular, they found that the RDCs involving the deoxyribose ring were not adequately fit by a single model. To compensate for this, separate structures were generated with the deoxyribose rings respectively restrained in either a C2′ endo or C3′ endo conformation. A fit to the relevant RDC measurements allowed the determination of site-specific populations for the sugar puckers.

4.6. Side-Chain Dynamics

The conformational flexibility and dynamics of protein side chains can play an important role in defining the interaction surfaces for the recognition of binding partners or by contributing to the entropic stabilization of the protein.[3] Due to the greater degrees of freedom available to side chains, it is correspondingly more difficult to separate contributions to RDCs that arise from dynamics versus conformational differences relative to a high-resolution structural model. Nevertheless, progress has been made in developing RDC-based probes for side-chain conformational heterogeneity and dynamics. Chou and Bax have described a simple method for the determination of χ_1 rotamers based on the measurement of one-bond $C^\beta-H^\beta$ RDCs in the absence of knowledge of backbone structure.[133] Their approach proceeds on the basis of comparison of measured $C^\beta-H^\beta$ RDCs with one-bond $C^\alpha-H^\alpha$ and $C^\alpha-C'$ RDCs, as well as $C^\alpha-N$ RDCs estimated from $^1D_{C^\alpha C'}$ couplings for the preceding residue. Because the $C^\beta-H^\beta$ bond will be parallel to one of the other three bonds for staggered rotamers, one can establish the rotameric state by direct comparison of the measured RDCs. Situations in which more than one rotameric state is significantly populated or the rotamer does not assume an ideal staggered geometry can be detected by lack of agreement of the $^1D_{C^\beta H^\beta}$ coupling with any of the other three measured couplings. A more extensive analysis of χ_1 torsion angle dynamics has been carried out by Mittermaier and Kay for the B1 domain of streptococcal protein L.[134] They utilized $^1D_{C^\beta H^\beta}$ RDCs in conjunction with refinement of the backbone conformation to accurately establish $C^\alpha-C^\beta$ bond orientations. Several different motional models were applied to the interpretation of their RDC data, with approximately 25% of residues fit much better by a model in which multiple rotamers were populated. A simple method for characterizing the dynamics of aromatic rings of phenylalanine or tyrosine residues has been proposed by Sprangers et al.[135] In an application to the SMN Tudor domain, the presence of dynamic averaging of the aromatic rings was suspected due to observed degeneracy of δ and ϵ chemical shifts. By comparison of $C^\beta-C^\gamma$ RDCs with one-bond aromatic $^{13}C-^1H$ RDCs, they established that two-site ring flips were occurring in all cases. Ring dynamics exhibiting higher symmetry could be excluded on the basis that, in that event, the measured aromatic $^{13}C-^1H$ RDCs would be equal to the measured $^1D_{C^\alpha C^\beta}$ couplings scaled by a factor of -0.125.

5. Future Perspectives

RDC techniques for characterizing motions spanning the picosecond to millisecond time scales have been steadily emerging in the past few years. There remains some disagreement as to the extent to which biomolecules are dynamic in nature, as well as the route best suited to study these motions. We have discussed here a number of different RDC-based approaches to the characterization of biomolecular dynamics, all of which have their own specific limitations. As such, discrepancies in results obtained using different methods do exist and should be taken as evidence that these tools are still evolving. The experimental characterization of protein dynamics is a difficult undertaking, and thus it is advantageous to have many different tools at our disposal. We anticipate that RDC-based methods for probing dynamics will continue to evolve and in the future be

employed increasingly in combination with some of the highly complementary NMR techniques for characterizing dynamics discussed in this edition.

6. Acknowledgments

We would like to thank Ananya Majumdar for critical reading of the manuscript. This work was supported by start up funds from the Krieger School of Arts and Sciences at Johns Hopkins University.

7. References

(1) Kay, L. E. *Nat. Struct. Biol.* **1998**, *5*, 513.
(2) Ishima, R.; Torchia, D. A. *Nat. Struct. Biol.* **2000**, *7*, 740.
(3) Wand, A. J. *Nat. Struct. Biol.* **2001**, *8*, 926.
(4) Palmer, A. G., 3rd; Kroenke, C. D.; Loria, J. P. *Methods Enzymol.* **2001**, *339*, 204.
(5) Akke, M. *Curr. Opin. Struct. Biol.* **2002**, *12*, 642.
(6) Bruschweiler, R. *Curr. Opin. Struct. Biol.* **2003**, *13*, 175.
(7) Case, D. A. *Acc. Chem. Res.* **2002**, *35*, 325.
(8) Prestegard, J. H.; Tolman, J. R.; Al-Hashimi, H. M.; Andrec, M. In *Biological Magnetic Resonance*; Krishna, N. R., Berliner, L. J., Eds.; Plenum: New York, 1999; Vol. 17.
(9) Prestegard, J. H.; Al-Hashimi, H. M.; Tolman, J. R. *Q. Rev. Biophys.* **2000**, *33*, 371.
(10) Tjandra, N. *Struct. Folding Des.* **1999**, *7*, R205.
(11) Mollova, E. T.; Hansen, M. R.; Pardi, A. *J. Am. Chem. Soc.* **2000**, *122*, 11561.
(12) Bax, A.; Kontaxis, G.; Tjandra, N. In *Nuclear Magnetic Resonance of Biological Macromolecules, Part B*; James, T. L., Dötsch, V., Schmitz, U., Eds.; Methods in Enzymology, Vol. 339; Academic Press: San Diego, CA, 2001.
(13) Al-Hashimi, H. M.; Patel, D. J. *J. Biomol. NMR* **2002**, *22*, 1.
(14) Tolman, J. R. *Curr. Opin. Struct. Biol.* **2001**, *11*, 532.
(15) Tolman, J. R.; Al-Hashimi, H. M. *Annu. Rep. NMR Spectrosc.* **2003**, *51*, 105.
(16) Prestegard, J. H.; Bougault, C. M.; Kishore, A. I. *Chem. Rev.* **2004**, *104*, 3519.
(17) Prestegard, J. H.; Kishore, A. I. *Curr. Opin. Chem. Biol.* **2001**, *5*, 584.
(18) Koenig, B. W. *ChemBioChem* **2002**, *3*, 975.
(19) Simon, B.; Sattler, M. *Angew. Chem., Int. Ed.* **2002**, *41*, 437.
(20) Gronenborn, A. M. *C. R. Biol.* **2002**, *325*, 957.
(21) Gronenborn, A. M. *Biol. Magn. Reson.* **2003**, *20*, 231.
(22) Clore, G. M.; Schwieters, C. D. *Curr. Opin. Struct. Biol.* **2002**, *12*, 146.
(23) Bax, A. *Protein Sci.* **2003**, *12*, 1.
(24) Griesinger, C.; Meiler, J.; Peti, W. *Biol. Magn. Reson.* **2003**, *20*, 163.
(25) Griesinger, C.; Peti, W.; Meiler, J.; Bruschweiler, R. *Methods Mol. Biol. (Clifton, N. J.)* **2004**, *278*, 107.
(26) Blackledge, M. *Prog. Nucl. Magn. Reson. Spectrosc.* **2005**, *46*, 23.
(27) Prestegard, J. H.; Mayer, K. L.; Valafar, H.; Benison, G. C. *Methods Enzymol.* **2005**, *394*, 175.
(28) Bastiaan, E. W.; MacLean, C.; Zijl, P. C. M. v.; Bothner-By, A. A. *Annu. Rep. NMR. Spectrosc.* **1987**, *19*, 35.
(29) *Molecular Orientation in High-Field High-Resolution NMR*; Bastiaan, E. W., MacLean, C., Eds.; Springer-Verlag: Berlin, 1990; Vol. 25.
(30) Gayathri, C.; Bothner-By, A. A.; van Zijl, P. C. M.; MacLean, C. *Chem. Phys. Lett.* **1982**, *87*, 192.
(31) van Zijl, P. C. M.; Ruessink, B. H.; Bulthuis, J.; MacLean, C. *Acc. Chem. Res.* **1984**, *17*, 172.
(32) Emsley, I. W.; Lindon, J. C. *NMR Spectroscopy Using Liquid Crystal Solvents*; Pergamon Press: Oxford, U.K., 1975.
(33) Diehl, P.; Khetrapal, C. L. *NMR: Basic Principles and Progress*; Springer-Verlag: New York, 1969.
(34) Khetrapal, C. L., Kunwar, A. C., Tracey, A. G., Diehl, P., Eds.; Springer-Verlag: Berlin, 1975; Vol. 9.
(35) Snyder, L. C. *J. Chem. Phys.* **1965**, *43*, 4041.
(36) Saupe, A. *Angew. Chem., Int. Ed. Engl.* **1968**, *7*, 97.
(37) Lohman, J. A. B.; MacLean, C. *Chem. Phys.* **1978**, *35*, 269.
(38) Bothner-By, A. A. In *Encyclopedia of Nuclear Magnetic Resonance*; Grant, D. M., Harris, R. K., Eds.; Wiley: Chichester, U.K., 1995.
(39) Emsley, J. W.; Foord, E. K.; Gandy, P. J. F.; Turner, D. L.; Zimmermann, H. *Liq. Cryst.* **1994**, *17*, 303.
(40) Emsley, J. W.; Heaton, N. J.; Kimmings, M. K.; Longeri, M. *Mol. Phys.* **1987**, *61*, 433.
(41) Emsley, J. W.; Luckhurst, G. R.; Stockley, C. P. *Mol. Phys.* **1981**, *44*, 565.
(42) Emsley, J. W.; Luckhurst, G. R. *Mol. Phys.* **1980**, *41*, 19.
(43) Burnell, E. E.; De Lange, C. A. *J. Magn. Reson.* **1980**, *39*, 461.
(44) Celebre, G.; Longeri, M.; Emsley, J. W. *Liq. Cryst.* **1989**, *6*, 689.
(45) Sinton, S. W.; Zax, D. B.; Murdoch, J. B.; Pines, A. *Mol. Phys.* **1984**, *53*, 333.
(46) Celebre, G.; Longeri, M.; Emsley, J. W. *Mol. Phys.* **1988**, *64*, 715.
(47) Emsley, J. W. *NMR of Liquid Crystals*; Reidel: Dordrecht, the Netherlands, 1985.
(48) Counsell, C. J. R.; Emsley, J. W.; Luckhurst, G. R.; Sachdev, H. S. *Mol. Phys.* **1988**, *63*, 33.
(49) Freed, J. H. *J. Chem. Phys.* **1977**, *66*, 4183.
(50) Rosen, M. E.; Rucker, S. P.; Schmidt, C.; Pines, A. *J. Phys. Chem.* **1993**, *97*, 3858.
(51) Emsley, J. W. In *Encyclopedia of NMR*; Grant, D. M., Harris, R. K., Eds.; John Wiley: Chichester, U.K., New York, 1996; Vol. 4.
(52) Emsley, J. W. In *Encyclopedia of NMR*; Grant, D. M., Harris, R. K., Eds.; John Wiley: Chichester, U.K., New York, 1996; Vol. 4.
(53) Abragam, A. *Principles of Nuclear Magnetism*; Clarendon Press: Oxford, U.K., 1961.
(54) Ernst, R. R.; Bodenhausen, G.; Wokaun, A. *Principles of Nuclear Magnetic Resonance in One and Two Dimensions*; Clarendon Press: Oxford, U.K., 1987.
(55) Case, D. A. *J. Biomol. NMR* **1999**, *15*, 95.
(56) Saupe, A. *Z. Naturforsh.* **1964**, *19a*, 161.
(57) Louhivuori, M.; Fredriksson, K.; Paeaekkoenen, K.; Permi, P.; Annila, A. *J. Biomol. NMR* **2004**, *29*, 517.
(58) Fredriksson, K.; Louhivuori, M.; Permi, P.; Annila, A. *J. Am. Chem. Soc.* **2004**, *126*, 12646.
(59) Bernado, P.; Blackledge, M. *J. Am. Chem. Soc.* **2004**, *126*, 7760.
(60) Bernado, P.; Blackledge, M. *J. Am. Chem. Soc.* **2004**, *126*, 4907.
(61) Bouvignies, G.; Bernado, P.; Blackledge, M. *J. Magn. Reson.* **2005**, *173*, 328.
(62) Deschamps, M.; Campbell, I. D.; Boyd, J. *J. Magn. Reson.* **2005**, *172*, 118.
(63) Losonczi, J. A.; Prestegard, J. H. *Biochemistry* **1998**, *37*, 706.
(64) Tolman, J. R.; Al-Hashimi, H. M.; Kay, L. E.; Prestegard, J. H. *J. Am. Chem. Soc.* **2001**, *123*, 1416.
(65) Tolman, J. R. *J. Am. Chem. Soc.* **2002**, *124*, 12020.
(66) Briggman, K. B.; Tolman, J. R. *J. Am. Chem. Soc* **2003**, *125*, 10164.
(67) Tolman, J. R.; Flanagan, J. M.; Kennedy, M. A.; Prestegard, J. H. *Proc. Natl. Acad. Sci. U.S.A.* **1995**, *92*, 9279.
(68) Tjandra, N.; Bax, A. *Science* **1997**, *278*, 1111.
(69) Tycko, R.; Blanco, F. J.; Ishii, Y. *J. Am. Chem. Soc.* **2000**, *122*, 9340.
(70) Sass, H.-J.; Musco, G.; Stahl, S. J.; Wingfield, P. T.; Grzesiek, S. *J. Biomol. NMR* **2000**, *18*, 303.
(71) Ishii, Y.; Markus, M. A.; Tycko, R. *J. Biomol. NMR* **2001**, *21*, 141.
(72) Chou, J. J.; Gaemers, S.; Howder, B.; Louis, J. M.; Bax, A. *J. Biomol. NMR* **2001**, *21*, 377.
(73) Ruckert, M.; Otting, G. *J. Am. Chem. Soc.* **2000**, *122*, 7793.
(74) Burnell, E. E.; de Lange, C. A. *Chem. Rev.* **1998**, *98*, 2359.
(75) Zweckstetter, M.; Bax, A. *J. Am. Chem. Soc.* **2000**, *122*, 3791.
(76) Fernandes, M. X.; Bernado, P.; Pons, M.; de la Torre, J. G. *J. Am. Chem. Soc.* **2001**, *123*, 12037.
(77) Almond, A.; Axelsen, J. B. *J. Am. Chem. Soc.* **2002**, *124*, 9986.
(78) Azurmendi, H. F.; Bush, C. A. *J Am Chem Soc* **2002**, *124*, 2426.
(79) Zweckstetter, M.; Hummer, G.; Bax, A. *Biophys. J.* **2004**, *86*, 3444.
(80) Press, W. H.; Teukolsky, S. A.; Vetterling, W. T.; Flannerygfdg, B. P. *Numerical recepies in C*; Cambridge University Press: Cambridge, U.K., 1992.
(81) Albert, A. *Regression and the Moore-Penrose Pseudoinverse*; Academic Press: New York, 1972.
(82) Ben-Israel, A.; Greville, T. N. E. *Generalized Inverses: Theory and Applications*; John Wiley & Sons: New York, 1974.
(83) Losonczi, J. A.; Andrec, M.; Fischer, M. W. F.; Prestegard, J. H. *J. Magn. Reson.* **1999**, *138*, 334.
(84) Moltke, S.; Grzesiek, S. *J. Biomol. NMR* **1999**, *15*, 77.
(85) Ulmer, T. S.; Ramirez, B. E.; Delaglio, F.; Bax, A. *J. Am. Chem. Soc.* **2003**, *125*, 9179.
(86) Hus, J.-C.; Brueschweiler, R. *J. Biomol. NMR* **2002**, *24*, 123.
(87) Hus, J.-C.; Peti, W.; Griesinger, C.; Brueschweiler, R. *J. Am. Chem. Soc.* **2003**, *125*, 5596.
(88) Tolman, J. R.; Flanagan, J. M.; Kennedy, M. A.; Prestegard, J. H. *Nat. Struct. Biol.* **1997**, *4*, 292.
(89) Bax, A.; Tjandra, N. *Nat. Struct. Biol.* **1997**, *4*, 254.
(90) Fischer, M. W. F.; Losonczi, J. A.; Weaver, J. L.; Prestegard, J. H. *Biochemistry* **1999**, *38*, 9013.
(91) Skrynnikov, N. R.; Goto, N. K.; Yang, D. W.; Choy, W. Y.; Tolman, J. R.; Mueller, G. A.; Kay, L. E. *J. Mol. Biol.* **2000**, *295*, 1265.
(92) Zhang, Q.; Throolin, R.; Pitt, S. W.; Serganov, A.; Al-Hashimi, H. M. *J. Am. Chem. Soc.* **2003**, *125*, 10530.
(93) Braddock, D. T.; Cai, M. L.; Baber, J. L.; Huang, Y.; Clore, G. M. *J. Am. Chem. Soc.* **2001**, *123*, 8634.

(94) Clore, G. M.; Gronenborn, A. M.; Bar, A. *J. Magn. Reson.* **1998**, *133*, 216.
(95) Braddock, D. T.; Louis, J. M.; Baber, J. L.; Levens, D.; Clore, G. M. *Nature* **2002**, *415*, 1051.
(96) Jacobs, D. M.; Saxena, K.; Vogtherr, M.; Bernado, P.; Pons, M.; Fiebig, K. M. *J. Biol. Chem.* **2003**, *278*, 26174.
(97) Ulmer, T. S.; Werner, J. M.; Campbell, I. D. *Structure* **2002**, *10*, 901.
(98) Yu, L. P.; Gunasekera, A. H.; Mack, J.; Olejniczak, E. T.; Chovan, L. E.; Ruan, X. A.; Towne, D. L.; Lerner, C. G.; Fesik, S. W. *J. Mol. Biol.* **2001**, *311*, 593.
(99) Lukin, J. A.; Kontaxis, G.; Simplaceanu, V.; Yuan, Y.; Bax, A.; Ho, C. *Proc. Natl. Acad. Sci. U.S.A.* **2003**, *100*, 517.
(100) Varadan, R.; Walker, O.; Pickart, C.; Fushman, D. *J. Mol. Biol.* **2002**, *324*, 637.
(101) Goto, N. K.; Skrynnikov, N. R.; Dahlquist, F. W.; Kay, L. E. *J. Mol. Biol.* **2001**, *308*, 745.
(102) Evenas, J.; Tugarinov, V.; Skrynnikov, N. R.; Goto, N. K.; Muhandiram, R.; Kay, L. E. *J. Mol. Biol.* **2001**, *309*, 961.
(103) Al-Hashimi, H. M.; Pitt, S. W.; Majumdar, A.; Xu, W.; Patel, D. J. *J. Mol. Biol.* **2003**, *329*, 867.
(104) Pitt, S. W.; Majumdar, A.; Serganov, A.; Patel, D. J.; Al-Hashimi, H. M. *J. Mol. Biol.* **2004**, *338*, 7.
(105) Pitt, S. W.; Zhang, Q.; Patel, D. J.; Al-Hashimi, H. M. *Angew. Chem., Int. Ed.* **2005**, *44*, 3412.
(106) Bertini, I.; Del Bianco, C.; Gelis, I.; Katsaros, N.; Luchinat, C.; Parigi, G.; Peana, M.; Provenzani, A.; Zoroddu, M. A. *Proc. Natl. Acad. Sci. U.S.A.* **2004**, *101*, 6841.
(107) Chou, J. J.; Li, S. P.; Klee, C. B.; Bax, A. *Nat. Struct. Biol.* **2001**, *8*, 990.
(108) van Buuren, B. N. M.; Schleucher, J.; Wittmann, V.; Griesinger, C.; Schwalbe, H.; Wijmenga, S. S. *Angew. Chem., Int. Ed.* **2004**, *43*, 187.
(109) Bryce, D. L.; Boisbouvier, J.; Bax, A. *J. Am. Chem. Soc.* **2004**, *126*, 10820.
(110) O'Neil-Cabello, E.; Bryce, D. L.; Nikonowicz, E. P.; Bax, A. *J. Am. Chem. Soc.* **2004**, *126*, 66.
(111) Zweckstetter, M.; Bax, A. *J. Biomol. NMR* **2002**, *23*, 127.
(112) Bryce, D. L.; Bax, A. *J. Biomol. NMR* **2004**, *28*, 273.
(113) Wang, L. C.; Pang, Y. X.; Holder, T.; Brender, J. R.; Kurochkin, A. V.; Zuiderweg, E. R. P. *Proc. Natl. Acad. Sci. U.S.A.* **2001**, *98*, 7684.
(114) Arumugam, S.; Gao, G.; Patton, B. L.; Semenchenko, V.; Brew, K.; Van Doren, S. R. *J. Mol. Biol.* **2003**, *327*, 719.
(115) Delaglio, F.; Kontaxis, G.; Bax, A. *J. Am. Chem. Soc.* **2000**, *122*, 2142.
(116) Ulmer, T. S.; Bax, A.; Cole, N. B.; Nussbaum, R. L. *J. Biol. Chem.* **2005**, *280*, 9595.
(117) Ding, K.; Louis, J. M.; Gronenborn, A. M. *J. Mol. Biol.* **2004**, *335*, 1299.
(118) Bertini, I.; Calderone, V.; Cosenza, M.; Fragai, M.; Lee, Y.-M.; Luchinat, C.; Mangani, S.; Terni, B.; Turano, P. *Proc. Natl. Acad. Sci. U.S.A.* **2005**, *102*, 5334.
(119) Lipari, G.; Szabo, A. *J. Am. Chem. Soc.* **1982**, *104*, 4546.
(120) Ramirez, B. E.; Bax, A. *J. Am. Chem. Soc.* **1998**, *120*, 9106.
(121) Al-Hashimi, H. M.; Valafar, H.; Terrell, M.; Zartler, E. R.; Eidsness, M. K.; Prestegard, J. H. *J. Magn. Reson.* **2000**, *143*, 402.
(122) Meiler, J.; Prompers, J. J.; Peti, W.; Griesinger, C.; Bruschweiler, R. *J. Am. Chem. Soc.* **2001**, *123*, 6098.
(123) Peti, W.; Meiler, J.; Bruschweiler, R.; Griesinger, C. *J. Am. Chem. Soc.* **2002**, *124*, 5822.
(124) Meiler, J.; Peti, W.; Griesinger, C. *J. Am. Chem. Soc.* **2003**, *125*, 8072.
(125) Vijaykumar, S.; Bugg, C. E.; Cook, W. J. *J. Mol. Biol.* **1987**, *194*, 531.
(126) Tjandra, N.; Feller, S. E.; Pastor, R. W.; Bax, A. *J. Am. Chem. Soc.* **1995**, *117*, 12562.
(127) Bremi, T.; Brüschweiler, R. *J. Am. Chem. Soc.* **1997**, *119*, 6672.
(128) Lienin, S. F.; Bremi, T.; Brutscher, B.; Bruschweiler, R.; Ernst, R. R. *J. Am. Chem. Soc.* **1998**, *120*, 9870.
(129) Brueschweiler, R.; Wright, P. E. *J. Am. Chem. Soc.* **1994**, *116*, 8426.
(130) Clore, G. M.; Schwieters, C. D. *J. Am. Chem. Soc.* **2004**, *126*, 2923.
(131) Clore, G. M.; Schwieters, C. D. *Biochemistry* **2004**, *43*, 10678.
(132) Wu, Z.; Delaglio, F.; Tjandra, N.; Zhurkin, V. B.; Bax, A. *J. Biomol. NMR* **2003**, *26*, 297.
(133) Chou, J. J.; Bax, A. *J. Am. Chem. Soc.* **2001**, *123*, 3844.
(134) Mittermaier, A.; Kay, L. E. *J. Am. Chem. Soc.* **2001**, *123*, 6892.
(135) Sprangers, R.; Groves, M. R.; Sinning, I.; Sattler, M. *J. Mol. Biol.* **2003**, *327*, 507.
(136) Ottiger, M.; Bax, A. *J. Biomol. NMR* **1998**, *12*, 361.
(137) Losonczi, J. A.; Prestegard, J. H. *J. Biomol. NMR* **1998**, *12*, 447.
(138) Wang, H.; Eberstadt, M.; Olejniczak, E. T.; Meadows, R. P.; Fesik, S. W. *J. Biomol. NMR* **1998**, *12*, 443.
(139) Ottiger, M.; Bax, A. *J. Biomol. NMR* **1999**, *13*, 187.
(140) Cavagnero, S.; Dyson, H. J.; Wright, P. E. *J. Biomol. NMR* **1999**, *13*, 387.
(141) Hansen, M. R.; Mueller, L.; Pardi, A. *Nat. Struct. Biol.* **1998**, *5*, 1065.
(142) Hansen, M. R.; Hanson, P.; Pardi, A. *Methods Enzymol.* **2000**, *317*, 220.
(143) Clore, G. M.; Starich, M. R.; Gronenborn, A. M. *J. Am. Chem. Soc.* **1998**, *120*, 10571.
(144) Barrientos, L. G.; Louis, J. M.; Gronenborn, A. M. *J. Magn. Reson.* **2001**, *149*, 154.
(145) Sass, J.; Cordier, F.; Hoffmann, A.; Cousin, A.; Omichinski, J. G.; Lowen, H.; Grzesiek, S. *J. Am. Chem. Soc.* **1999**, *121*, 2047.
(146) Koenig, B. W.; Hu, J. S.; Ottiger, M.; Bose, S.; Hendler, R. W.; Bax, A. *J. Am. Chem. Soc.* **1999**, *121*, 1385.
(147) Bernado, P.; Barbieri, R.; Padros, E.; Luchinat, C.; Pons, M. *J. Am. Chem. Soc.* **2002**, *124*, 374.
(148) Fleming, K.; Gray, D.; Prasannan, S.; Matthews, S. *J. Am. Chem. Soc.* **2000**, *122*, 5224.
(149) Valafar, H.; Mayer, K. L.; Bougault, C. M.; LeBlond, P. D.; Jenney, F. E., Jr.; Brereton, P. S.; Adams, M. W. W.; Prestegard, J. H. *J. Struct. Funct. Genomics* **2004**, *5*, 241.
(150) Barrientos, L. G.; Gawrisch, K.; Cheng, N.; Steven, A. C.; Gronenborn, A. M. *Langmuir* **2002**, *18*, 3773.
(151) Barrientos, L. G.; Dolan, C.; Gronenborn, A. M. *J. Biomol. NMR* **2000**, *16*, 329.
(152) Prosser, R. S.; Losonczi, J. A.; Shiyanovskaya, I. V. *J. Am. Chem. Soc.* **1998**, *120*, 11010.
(153) Bertini, I.; Felli, I. C.; Luchinat, C. *J. Biomol. NMR* **2000**, *18*, 347.
(154) Feeney, J.; Birdsall, B.; Bradbury, A. F.; Biekofsky, R. R.; Bayley, P. M. *J. Biomol. NMR* **2001**, *21*, 41.
(155) Ma, C.; Opella, S. J. *J. Magn. Reson.* **2000**, *146*, 381.
(156) Woehnert, J.; Franz, K. J.; Nitz, M.; Imperiali, B.; Schwalbe, H. *J. Am. Chem. Soc.* **2003**, *125*, 13338.
(157) Meier, S.; Haeussinger, D.; Grzesiek, S. *J. Biomol. NMR* **2002**, *24*, 351.
(158) Trempe, J. F.; Morin, F. G.; Xia, Z. C.; Marchessault, R. H.; Gehring, K. *J. Biomol. NMR* **2002**, *22*, 83.
(159) Riley, S. A.; Giuliani, J. R.; Augustine, M. P. *J. Magn. Reson.* **2002**, *159*, 82.

CR040429Z